

## Petrogenesis of main group pallasite meteorites based on relationships among texture, mineralogy, and geochemistry

Seann J. McKIBBIN <sup>1,5,6\*</sup>, Lidia PITTARELLO <sup>1,7</sup>, Christina MAKARONA<sup>1</sup>,  
Christopher HAMANN <sup>2,3</sup>, Lutz HECHT<sup>2,3</sup>, Stepan M. CHERNONOZHKIN<sup>4,8</sup>, Steven GODERIS<sup>1</sup>,  
and Philippe CLAEYS <sup>1</sup>

<sup>1</sup>Analytical, Environmental and Geo-Chemistry, Vrije Universiteit Brussel, Pleinlaan 2, Brussels 1050, Belgium

<sup>2</sup>Museum für Naturkunde, Leibniz-Institut für Evolutions- und Biodiversitätsforschung, Invalidenstraße 43,  
10115 Berlin, Germany

<sup>3</sup>Institut für Geologische Wissenschaften, Freie Universität Berlin, Malteserstraße 74-100, 12249 Berlin, Germany

<sup>4</sup>GeoRessources, Faculté des Sciences et Technologies, Université de Lorraine, Rue Jacques Callot, BP 70239, 54506,  
Vandoeuvre-lès-Nancy CEDEX, France

<sup>5</sup>Present address: Institut für Erd- und Umweltwissenschaften, Universität Potsdam, Haus 27, Karl-Liebknecht-Straße 24-25,  
Potsdam-Golm 14476, Germany

<sup>6</sup>Present address: Geowissenschaftliches Zentrum, Abteilung Isotopengeologie, Georg-August-Universität Göttingen,  
Goldschmidtstraße 1, Göttingen 37073, Germany

<sup>7</sup>Present address: Department of Lithospheric Research, Universität Wien, UZA 2, Althanstraße 14, Vienna A-1090, Austria

<sup>8</sup>Present address: Department of Chemistry, Universiteit Gent, Krijgslaan 281-S12, Ghent 9000, Belgium

\*Corresponding author. E-mail: seann.mckibbin@gmail.com

(Received 23 September 2018; revision accepted 17 August 2019)

**Abstract**—Main group pallasite meteorites are samples of a single early magmatic planetesimal, dominated by metal and olivine but containing accessory chromite, sulfide, phosphide, phosphates, and rare phosphoran olivine. They represent mixtures of core and mantle materials, but the environment of formation is poorly understood, with a quiescent core–mantle boundary, violent core–mantle mixture, or surface mixture all recently suggested. Here, we review main group pallasite data sets and petrologic characteristics, and present new observations on the low-MnO pallasite Brahin that contains abundant fragmental olivine, but also rounded and angular olivine and potential evidence of sulfide–phosphide liquid immiscibility. A reassessment of the literature shows that low-MnO and high-FeO subgroups preferentially host rounded olivine and low-temperature P<sub>2</sub>O<sub>5</sub>-rich phases such as the Mg-phosphate farringtonite and phosphoran olivine. These phases form after metal and silicate reservoirs back-react during decreasing temperature after initial separation, resulting in oxidation of phosphorus and chromium. Farringtonite and phosphoran olivine have not been found in the common subgroup PMG, which are mechanical mixtures of olivine, chromite with moderate Al<sub>2</sub>O<sub>3</sub> contents, primitive solid metal, and evolved liquid metal. Lower concentrations of Mn in olivine of the low-MnO PMG subgroup, and high concentrations of Mn in low-Al<sub>2</sub>O<sub>3</sub> chromites, trace the development and escape of sulfide-rich melt in pallasites and the partially chalcophile behavior for Mn in this environment. Pallasites with rounded olivine indicate that the core–mantle boundary of their planetesimal may not be a simple interface but rather a volume in which interactions between metal, silicate, and other components occur.

### INTRODUCTION

Naturally delivered samples of differentiated planetesimals, formed in the first few million years of

the solar system's history, are available to us as nonchondritic meteorites. However, these physical records are overwhelmingly represented by metallic meteoritic sources with far fewer samples of unique

mantles and crusts (in the ranges 26–60 versus 4–18 parent bodies, respectively; e.g., Bell et al. 1989; Greenwood et al. 2015). Associated with this is a scarcity of sulfide-rich meteorites that should have crystallized abundant troilite via differentiation of metallic liquids, but these might be highly vulnerable to destruction during transport, atmospheric entry, or during residence on the surface of the Earth (Kracher and Wasson 1982). Alternately, sulfide might have been sequestered deep inside planetesimal cores and be unsuitably located for transport to Earth as meteorites (e.g., Boesenberg et al. 2012).

Although processes of differentiation leading to separate planetesimal cores and mantles are poorly recorded by meteorites, the final stages of core–mantle separation are preserved in a few planetary sources, particularly the various pallasite parent bodies. Pallasite meteorites consist predominantly of mixtures of olivine and metal with accessory troilite, chromite, phosphide, and various phosphate minerals (Boesenberg et al. 2012). Most are geochemically, isotopically, and petrologically related, earning them the designation “main group” pallasite (hereafter PMG following Wasson and Choi 2003). In particular, their coherent triple-oxygen isotope systematics strongly indicate that the PMG originated from just one or possibly two well-sampled parent bodies (Greenwood et al. 2015; Ali et al. 2018). However, just as the number of recognized planetesimal sources of crustal, basaltic rocks has increased in recent years (Scott et al. 2009; Sanborn and Yin 2014), so have multiple pallasite parent bodies been recognized by significant differences in oxygen isotope composition that cannot be related to each other through mass-dependent fractionation (e.g., Clayton and Mayeda 1978, 1996). These other bodies are poorly sampled, but illustrate the abundance of pallasite-producing planetesimals in the early solar system, with at least five distinct sources represented by the various groups or individual pallasites. These include the PMG; the Eagle Station group (PES after Wasson and Choi 2003); and the ungrouped or otherwise anomalous pallasites Milton (Jones et al. 2003), Vermillion, Yamato 8451 (Boesenberg et al. 2000), Choteau (Gregory et al. 2016), Zinder, Northwest Africa 1911 (Bunch et al. 2005), and Northwest Africa 10019 (Agee et al. 2015). These confirm that pallasitic material is frequently produced after partial or complete melting of primitive planetesimal mantles. For molten planetesimals, pallasitic material may represent the default, penultimate end product of differentiation, core–mantle separation, and final metal-silicate equilibration.

The available data for pallasites, long dominated by large petrographic and geochemical studies (Buseck 1977; Buseck and Holdsworth 1977; Scott 1977a, 1977b) have recently received interesting new contributions

from a variety of fields. Improvement in metallographic cooling rates (Yang et al. 2010), constraints on the stability and occurrence of unusual phosphorus-rich olivine (with more than ~1 wt%  $P_2O_5$  and hereafter referred to as “phosphoran olivine”; Boesenberg and Hewins 2010; Fowler-Gerace and Tait 2015), and new paleomagnetic histories (Tarduno et al. 2012; Bryson et al. 2015) have been brought to the literature. Each of these has driven its own, somewhat exclusive model of pallasite petrogenesis. The suggested formation environments include deep, thorough impact mixing zones of olivine and metal (Scott 2007; Yang et al. 2010), a quiescently evolving core–mantle boundary or olivine-metal zone (e.g., Boesenberg et al. 2012), and surface mixing of olivine and metal (Tarduno et al. 2012; Bryson et al. 2015). Recently, experimental work (Solferino et al. 2015) and new petrographic observations (Scott 2017) have indicated that the morphology of pallasite olivine, that is, the macroscale textures and grain size, was controlled by the presence of and their residence time in an Fe-S liquid. Fragmental olivines are therefore likely to have formed from relatively large (~5–15 mm) rounded or angular precursors, which are the most common morphological type observed in pallasites (Scott 1977b). Here, we investigate whether any previously unrecognized correlation exists between olivine morphology, olivine geochemistry, and accessory phase mineralogy in the PMG. Our study focuses on the fragmentally textured pallasite Brahin (e.g., Boesenberg et al. 2012), the relationship between it and the other members of the PMG, and the possible planetesimal environments responsible for the various pallasite subgroups.

## MOTIVATION, SAMPLE SELECTION, AND METHODS

Within the PMG, Boesenberg et al. (2012) highlighted the difficulty of identifying coherent subgroups that gather all textural, mineralogical, and geochemical features together. The geochemical information available for olivine is particularly scarce, with Mn being the only trace element that has been collected systematically. The Fe-Mg-Mn systematics of PMG olivine define a subgroup (hereafter referred to as “low-MnO PMG”) with MnO contents in olivine lower than ~0.25 wt% (e.g., Boesenberg et al. 2012). We will refer to the main cluster of PMG with similar olivine major element compositions of ~Fa<sub>12-13</sub> and with ~0.30 wt% MnO as the “common subgroup PMG.” The low-MnO PMG subgroup includes Brahin, Brenham, Hambleton, Krasnojarsk, Molong, Sericho, Seymchan, and Thiel Mountains (Smith et al. 1983; Mittlefehldt et al. 1998; Wasson et al. 1999; Hsu 2003; Boesenberg

et al. 2012, 2018; Ali et al. 2018). The olivines in Brenham, Krasnojarsk, and Thiel Mountains seem to be exclusively of the rounded variety (Buseck 1977; Scott 1977b). The olivines in the heavily corroded Molong pallasite (Mingaye 1916) were described as predominantly angular although with other types present (Buseck 1977) but were specifically identified as having potentially originated from a Brenham-like precursor by separation of olivine grains because of the presence of some rounded olivine (Scott 1977b). Similarly, Sericho has been reported to contain rounded and occasionally polyhedral grains (Boesenberg et al. 2018). The olivine in Seymchan is diverse, including rounded, angular, and fragmental grains (Van Niekerk et al. 2007; Yang et al. 2010; Boesenberg et al. 2012). By contrast, Hambleton has been reported to contain angular and abundant fragmental olivine, and is anomalous in its very high sulfide content (Johnson et al. 2006a, 2006b). Brahin has been described on the macroscale as fragmental (Buseck 1977) and as containing both highly angular olivine fragments as well as large angular olivine grains (Scott 1977b). Brahin and Hambleton are therefore the only low-MnO PMG that have not been reported to contain some rounded olivine. Brahin is also of interest as one of the few PMG to contain phosphoran olivine (Buseck 1977) and silico-phosphate (Buseck and Holdsworth 1977).

Because Brahin contains geochemically similar olivine but a conspicuous fragmental appearance compared with that of other low-MnO PMG, sections of this pallasite were investigated at the Royal Belgian Institute of Natural Sciences, Brussels, Belgium (RBINS). A piece has been identified measuring  $\sim 5 \times 5$  cm (RBINS sample M226) with approximately half containing relatively abundant large rounded olivine, with most  $\sim 4$ – $5$  mm and up to  $\sim 6$  mm diameter, while the rest contains finer angular and fragmental olivine with a wide range of grain sizes that is more typical of this meteorite. This petrographic arrangement has not been reported previously in Brahin and the section was therefore mapped by microscale X-ray fluorescence (micro-XRF) using a Bruker M4. By comparison with other methods (e.g., backscatter electron imaging by scanning electron microscopy), this method enables a larger field of view, requires no sample preparation, and is also nondestructive. Our system is equipped with a 30 W Rh-anode X-ray source with a Be side-window, and two silicon drift detector spectrometers with detector areas of  $30 \text{ mm}^2$ , located symmetrically with respect to the sample and X-ray source (energy resolution of 145 eV for Mn  $K_{\alpha}$ ). The source was run at an operating voltage of 50 kV and current 600  $\mu\text{A}$  and the sample was held under vacuum (20 mbar). The Bruker M4 Tornado software was used to generate a

false color phase map from the obtained four-dimensional “data-block” ( $x$ ,  $y$ , and  $K_{\alpha}$  intensity for all detected elements; Fig. 1a). The simplified accessory phase map was manually traced by hand and represents an interpretation map excluding olivine and metal (Fig. 1b).

The aforementioned preferential association of rounded olivine morphology, anomalous (i.e., low-MnO PMG) olivine composition, and phosphorus-rich phases has also prompted us to obtain quantitative major and minor element analyses of olivine in several PMG by electron microprobe analysis (EMPA). We analyzed olivine in Brenham (from the Research School of Earth Sciences, Australian National University); Cumulus Ridge 04071,23 (from the Meteorite Working Group, NASA Astromaterials Curation; hereafter referred to as CMS 04071); Esquel and Imilac (from RBINS, samples M218 and M222); and Brahin, Fukang, and Seymchan (from private dealers). The piece of Seymchan we investigated contains only angular and minor fragmental olivine, but rounded olivine has also been reported (Yang et al. 2010; Kichanov et al. 2018). The other samples in our study are petrographically similar to previous reports for these meteorites. There are few complete EMPA analyses available for olivine from Brahin, CMS 04071, Esquel, Fukang, and Seymchan in the literature, that is, analyses that include MnO. There are more data available for Brenham and Imilac and these serve as a check on our analyses.

Quantitative analysis of olivine cores was made with a JEOL JXA-8500F field-emission electron microprobe (Museum für Naturkunde, Berlin, Germany) with a fully focused beam of 50 nA current with 15 kV accelerating voltage, utilizing five wavelength-dispersive X-ray spectrometers. New calibrations were made using Astimex and Smithsonian reference materials.  $K_{\alpha}$  peak measurements were made for Si, Al, Mg, P (TAP), Ti, Mn, (PETJ), Ni, Ca, (PETH), Cr, and Fe (LIFH) with backgrounds measured on both sides of each peak. Spectrometer arrangement and measurement times are given in Table 1. Matrix effects were corrected using the JEOL inbuilt ZAF routine. These are the same instrumental settings as previously reported in Chernonozhkin et al. (2017).

## RESULTS AND OBSERVATIONS

### Micro-XRF Mapping and Petrographic Observations

Our micro-XRF map illustrates a range of olivine morphologies in the studied piece of Brahin (Fig. 1a). All olivine grains are set in a groundmass of metal or accessory phases. Large (up to  $\sim 6$  mm) rounded olivines

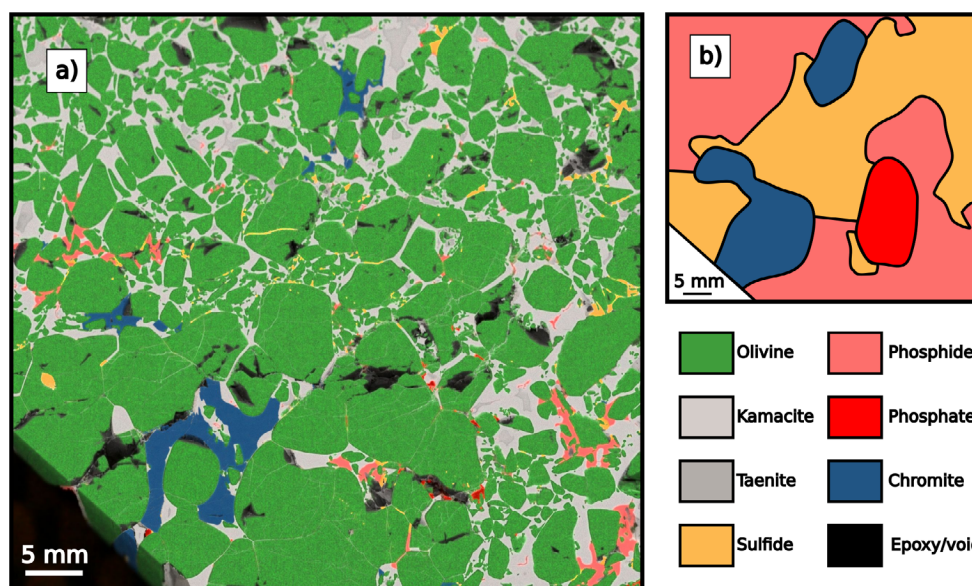


Fig. 1. a) Micro-XRF false color phase map of Brahin pallasite section (sample RBINS M226) with typical Brahin fragmentally textured olivine in upper half and previously unrecognized rounded and rare polygonally textured olivine in lower half. Field of view ~50 mm. Green = olivine; gray = Fe-Ni metal; blue = chromite; yellow = sulfide; pink = phosphide; red = phosphate; black = epoxy filled hole or no sample. b) Simplified accessory phase map indicating areas dominated by a single accessory phase coexisting with the major phases olivine, kamacite, and taenite. (Color figure can be viewed at [wileyonlinelibrary.com](http://wileyonlinelibrary.com).)

Table 1. WDS spectrometer arrangement and measurement times for  $K_{\alpha}$  peak measurements by EMPA in pallasite olivine.

Spectrometer	TAP	TAP	PETJ	PETH	LIFH
Element	Si	Mg	Ti	Ni	Cr
Peak (s)	20	20	40	30	40
Background 1	10	10	20	15	20
Background 2	10	10	20	15	20
	Al	P	Mn	Ca	Fe
Peak (s)	40	40	20	30	20
Background 1	20	20	10	15	10
Background 2	20	20	10	15	10

only exhibit curvilinear margins along surfaces in contact with the groundmass. Large olivine crystals may have some contact with each other and where this occurs, their mutual boundaries are straight; some crystals are sufficiently close-set to one another that they share triple junctions in section (lower middle of Fig. 1a). Some exhibit straight margins that match nearby grains, as though having been invaded by metal (middle of Fig. 1a), a feature most often observed in pallasites dominated by angular olivine or polycrystalline olivine aggregates. Midsized and fine-grained olivine crystals are more irregular in shape and have potentially high aspect ratios, indicative of intragranular fracture or fragmentation. However, almost all midsized and fine-grained olivine

have rounded corners to some degree, even where the macroscale morphology is angular. In association with olivine are occasional voids that resulted from plucking of olivine, which were later filled with epoxy resin and are represented in black (Fig. 1a). The bottom left corner was removed during the sample preparation of a previous study and this also appears as black.

In most of this section of Brahin, regions containing only a single accessory phase can be identified; therefore, in Fig. 1b, we present an interpretation map indicating our inferred domain boundaries for each accessory phase. Two large domains in which the only accessory phase is phosphide (upper left and lower right of Figs. 1a and 1b) and one in which it is sulfide (upper right and through the middle of Figs. 1a and 1b) host submillimeter scale grains of each phase that enclose fragmentally textured olivines or adjacent to large olivine grains. Chromite is present in two domains. The first is mostly as a millimeter scale, probably a continuous domain adjacent to olivine. The chromite does not contain distinctive faceted crystal edges, and rather occurs as curved masses that conform to the edge of the olivine (lower left of Figs. 1a and 1b; similar to massive chromite described by Wasson et al. [1999] for Brenham). The second chromite domain in this section is associated with fragmental olivine (upper middle of Figs. 1a and 1b). Although we cannot be sure that the two domains of phosphide and the two domains of chromite were not, respectively, connected in three

dimensions, the absence of these phases in other parts of the section indicates strong heterogeneity at the centimeter scale and possible continuity outside of the plane of the section. Rare phosphate is also present as submillimeter grains in a single domain in the lower right, surrounded by the large phosphide region (lower right of Figs. 1a and 1b). An additional phosphate grain occurs in association with the largest chromite.

### Olivine Geochemistry by EMPA

Our EMPA analyses of olivine for PMG olivine cores are in good agreement with previously published data (Tables 2 and 3; Smith et al. 1983; Wasson et al. 1999; Lauretta et al. 2006; Danielson et al. 2009; Boesenberg et al. 2012; Ali et al. 2018). We find similar values for the content of the fayalitic component ( $Fa\#$ , defined as molar  $Fe/[Fe+Mg] \times 100$ ) for olivine from these pallasites, with relatively low values for Brahin, Esquel, and Seymchan ( $\sim Fa_{11.5}$ ); intermediate values for Brenham, CMS 04071, and Imilac ( $\sim Fa_{12}$ ); and a higher value for Fukang ( $Fa_{13.7}$ ). The contents of MnO for Brahin and Brenham olivine are lower than the others (0.21 and 0.20 wt% versus average of 0.27 wt% for the common PMG samples). The MnO content we have found for angular olivine in Seymchan (0.26 wt%) is higher than that reported by Ali et al. (2018; 0.22 wt%), yielding molar Fe/Mn values that span the gap between common and low-MnO subgroups. Ali et al. (2018) do not indicate whether their olivine was of the angular, rounded, or fragmental variety, but this large discrepancy is consistent with differing MnO contents in the olivine of the same pallasite according to olivine morphology. We therefore tentatively suggest the possibility that Seymchan could be classified as “transitional” to the common and low-MnO PMG subgroups (Table 3).

Other minor elements are close to or below detection limit, but some are usefully resolved from zero (Table 2). We have found the  $Cr_2O_3$ , CaO, and  $Al_2O_3$  contents of PMG olivine to be correlated. In Esquel and Fukang, they are higher than the other pallasites, at 0.05, 0.025, and 0.02 wt%, respectively, while the others have values that decrease until close to or below detection limits (at approximately 0.010, 0.003, and 0.005 wt%, respectively; Table 2 and supporting information Table S1 in Data S1). We found the  $P_2O_5$  contents of olivine to be below the quantification limit (with analyses almost exclusively below 0.02 wt% and most below detection limit of  $\sim 0.011$  wt%; Table S1 in Data S1). We did not observe any phosphoran olivine (with  $\sim 1$  wt%  $P_2O_5$ ) in any of our samples. We do not report values for  $TiO_2$  or NiO because they are all very close to or below detection limit (approximately 0.009 and 0.010 wt%, respectively).

All new data used to calculate the average EMPA compositions in Table 2 are given in Table S1 in Data S1. Our new olivine compositions have been incorporated into the full data set used to construct Fig. 2 (Table 3; Table S2 in Data S1). These analyses, in conjunction with observations from the large slab of Brahin that we investigated (Fig. 1) and our assessment of the literature (Table 3; Fig. 2a), establish a new constraint on pallasite petrogenesis: that pallasites in the low-MnO olivine subgroup of PMG have partly or exclusively “rounded” primary olivine textures. In the next section, we will show that morphologies and compositions of olivine in the various PMG subgroups are also related to their accessory phase mineralogies.

## DISCUSSION

### Correlated Characteristics among the PMG Meteorites

#### *Olivine Morphology and Rounding*

There are three macroscale occurrences of olivine in PMG meteorites and the relationships between the various types have only recently become clear. In the first occurrence, relatively large (commonly  $\sim 5$  mm diameter and up to  $\sim 5$ – $15$  mm diameter; Scott 1977b) rounded olivine exhibits a restricted range of grain sizes and often occurs such that grains are partly isolated from each other by metal or other groundmass phases. On a microscale, the olivine margins of many pallasites including those of the other petrographic types also exhibit roundness (e.g., Buseck 1977). In the second occurrence, angular, equiaxed grains may exhibit a larger range in grain size (up to  $\sim 25$  mm or even larger; Scott 1977b). Where adjacent to each other, they have been considered “equilibrated” or in “textural equilibrium,” sharing triple junctions in cross section (e.g., Buseck 1977; Scott 1977b). Larger assemblages of angular olivine also occur and have been referred to as aggregates and in rare cases as masses or clusters (Scott 1977b; Boesenberg et al. 2012). These may have undergone intergranular fracture and greater or lesser degrees of gentle or more vigorous separation with the space between now filled with metal or an accessory mineral. Finally, fragmental or “highly angular” olivine shards exhibit a wide range of grain sizes and were inferred to form by intragranular fracture. We use the angular, rounded, and fragmental (A, R, F) terminology of Buseck (1977) for the macroscale textures of pallasites and assign each PMG one or more of these signifiers (the full details of our textural assignments are given in Table S3 in Data S1). We have conservatively attributed each signifier even on the basis of only a few reported grains of each type, or a brief mention in the description given in any particular publication. This may be of particular interest for pallasites dominated by angular

Table 2. Average EMPA compositions for PMG olivine cores.

Sample	Brahin ( <i>n</i> = 16)		Brenham ( <i>n</i> = 18)		CMS 04071 ( <i>n</i> = 19)		Esquel ( <i>n</i> = 31)		Fukang ( <i>n</i> = 16)		Imilac ( <i>n</i> = 20)		Seymchan ( <i>n</i> = 19)	
SiO <sub>2</sub>	40.15	0.12	39.96	0.13	39.87	0.17	40.17	0.12	39.84	0.07	40.20	0.09	40.00	0.17
Al <sub>2</sub> O <sub>3</sub>	0.004	0.004	0.002	0.003	0.001	0.002	0.024	0.007	0.022	0.006	0.009	0.006	0.002	0.003
Cr <sub>2</sub> O <sub>3</sub>	0.015	0.008	0.017	0.008	0.014	0.009	0.052	0.013	0.044	0.016	0.024	0.008	0.015	0.008
FeO	10.98	0.08	11.60	0.10	11.55	0.08	11.14	0.09	13.20	0.06	11.77	0.07	10.78	0.05
MnO	0.205	0.009	0.195	0.011	0.252	0.010	0.271	0.009	0.309	0.015	0.275	0.017	0.256	0.015
MgO	48.19	0.19	48.25	0.14	48.25	0.18	47.79	0.23	46.60	0.14	47.54	0.15	49.10	0.17
CaO	0.010	0.005	0.008	0.004	0.006	0.003	0.028	0.005	0.022	0.005	0.012	0.004	0.008	0.002
P <sub>2</sub> O <sub>5</sub>	0.007	0.007	0.008	0.006	0.009	0.008	0.004	0.005	0.002	0.003	0.005	0.005	0.006	0.005
Total	99.56		100.04		99.94		99.49		100.04		99.85		100.16	
Si	5.964	0.009	5.928	0.012	5.922	0.019	5.978	0.015	5.954	0.013	5.977	0.008	5.908	0.017
Al	0.001	0.001	0.000	0.000	0.000	0.000	0.004	0.001	0.004	0.001	0.002	0.001	0.000	0.001
Cr	0.002	0.001	0.002	0.001	0.002	0.001	0.006	0.002	0.005	0.002	0.003	0.001	0.002	0.001
Fe	1.365	0.008	1.439	0.011	1.435	0.010	1.386	0.011	1.650	0.008	1.464	0.007	1.332	0.006
Mn	0.026	0.001	0.025	0.001	0.032	0.001	0.034	0.001	0.039	0.002	0.035	0.002	0.032	0.002
Mg	10.672	0.020	10.672	0.023	10.683	0.035	10.601	0.028	10.383	0.026	10.536	0.021	10.813	0.033
Ca	0.002	0.001	0.001	0.001	0.001	0.000	0.004	0.001	0.003	0.001	0.002	0.001	0.001	0.000
P	0.001	0.001	0.001	0.001	0.001	0.001	0.001	0.001	0.000	0.000	0.001	0.001	0.001	0.001
Total	18.032		18.068		18.075		18.015		18.040		18.019		18.089	
Fa#	11.34	0.07	11.88	0.08	11.84	0.08	11.56	0.09	13.71	0.07	12.20	0.07	10.96	0.05
Fe/Mg	0.128	0.001	0.135	0.001	0.134	0.001	0.131	0.001	0.159	0.001	0.139	0.001	0.123	0.001
Fe/Mn	52.9	2.4	58.9	2.9	45.3	1.8	40.6	1.3	42.3	2.1	42.4	2.8	41.7	2.5

Values are expressed in wt%; SD.

olivine but with a few rounded olivines, for example, CMS 04071 (Danielson et al. 2009) and Fukang (Lauretta et al. 2006; DellaGiustina et al. 2011, 2019).

The original form of olivine in pallasites, at the time of olivine-metal mixing (if olivine represents a cumulate) or immediately after olivine grain growth (if refractory olivine and metal remain as restate after high degrees of melting) is of importance for constraining the histories of pallasite parent bodies. Early suggestions to explain pallasite textures favored rounding of initially fragmental or angular olivine, driven by the observation of microscale rounding of olivine in virtually all pallasites (Buseck 1977; Scott 1977b) that might occasionally proceed to high degrees. However, it has since been shown that olivine rounding in various liquids proceeds relatively quickly on geologic timescales, and faster in the presence of a metal-sulfide liquid than under subsolidus conditions (Ohtani 1983; Saiki et al. 2003; Guignard et al. 2012; Solferino et al. 2015). In the presence of substantial sulfide melt, the rounding of olivine on a macroscale is possible over timescales on the order of a few hundred thousand years (Solferino et al. 2015). Along with the occasional occurrence of more than one textural type of olivine in a single pallasite (e.g., Boesenberg et al. 2012), this rules out the possibility of fragmental olivine as a precursor for other types of pallasite olivine (although angular olivine could conceivably become rounded, and ultimately the very earliest form of large olivine might

even have been euhedral in the likely case that it formed in the presence of a silicate melt, e.g., Scott 2017). Additionally, these rapid timescales for rounding indicate that separate sources or environments are required for pallasites dominated by rounded olivine, and for those by angular or polycrystalline olivine masses. According to Solferino et al. (2015), it seems that the main control is whether any particular olivine grain was exposed to melt or shared a boundary with other olivine grains. In the former case, olivine would develop conspicuous rounded surfaces where they were exposed to metallic liquid, while in the latter case, they would grow into dense dunitic masses (Scott 1977b). Slight separation of olivine, disintegration of olivine masses, and infiltration of metal occurred before final cooling. The primary, high-temperature silicate products of pallasitic environments are therefore rounded olivine and angular or polycrystalline olivine masses, which we refer to as the primary olivine or texture of pallasites. A combination of both rounded and angular olivine in a single pallasite indicates either a variable olivine-liquid ratio over the scale of sampling (as in the quiescent model of Boesenberg et al. 2012), or that mixing of olivine occurred across geological domains (as in the impact mixing model of Yang et al. 2010). Fragmental olivine is a secondary product formed by brittle deformation at high strain rates (Scott 1977b, 2017). In the following sections, we will connect these petrographic characteristics of primary rounded and

Table 3. PMG subgroups with characteristic examples.

PMG subgroup	Example	Predominant texture	Olivine		Mg-phosphate farringtonite?	Phosphoran olivine?
			Fa#	MnO		
Common	Admire	AF	12.0	0.27	–	–
	Ahumada	A	11.5	0.28	–	–
	Albin	F	12.5	–	–	–
	Argonia	AF	13.5	–	–	–
	CMS 04071	AR	12.0	0.27	–	–
	Esquel	A	11.6	0.30	–	–
	Finmarken	A	12.8	0.28	–	–
	Fukang	AR	13.7	0.31	–	–
	Glorieta Mountain	A	13.4	0.30	–	–
	Huckitta	F	12.0	0.26	–	–
	Imilac	AF	12.8	0.31	–	–
	Marjalahti	AF	11.4	0.29	–	–
	Mineo	AF	13.0	0.29	–	–
	Newport	AF	11.8	0.27	–	–
	Omolon	R	12.2	–	–	–
	Otinapa	AF	13.5	0.31	–	–
	Pallasovka	AF	12.6	0.27	–	–
Anomalous Transitional	Pavlodar	R	12.1	0.36	–	–
	Seymchan (high-MnO)	ARF	11.0	0.26	–	–
	Seymchan (low-MnO)		11.4	0.22	–	–
Low-MnO	Southampton	ARF	12.3	0.24	–	–
	Brahin	ARF	11.7	0.22	–	Yes
	Brenham	R	12.2	0.21	Yes	Yes
	Hambleton	AF	11.8	0.22	–	–
	Krasnojarsk	R	12.1	0.19	Yes	–
	Molong	AR	11.2	0.20	–	–
	Sericho	AR	12.6	0.21	–	–
	Thiel Mountains	R	12.1	0.21	–	–
High-FeO (PMG-as)	Phillips County	AR	18.5	–	Yes	–
	Rawlinna	R	16.5	–	Yes	Yes
	Springwater	R	17.7	0.32	Yes	Yes
	Sterley	–	17.2	0.31	–	–
	Zaisho	F	18.4	0.40	Yes	Yes

Olivine morphologies are classified according to: A = angular; R = rounded; F = fragmental. Olivine Fa# = molar  $100 \times \text{Fe}/(\text{Fe}+\text{Mg})$ ; MnO in wt% (all compositions from EMPA). Values given are averages calculated from those in the original studies and in this study, except Seymchan (high-MnO value from this study). Data from: Buseck (1977); Buseck and Holdsworth (1977); Scott (1977b); Shima et al. (1980); Smith et al. (1983); Buseck and Clark (1984); Mittlefehldt et al. (1998); Wasson and Choi (2003); Sadilenko et al. (2006); Sharygin et al. (2006); Haag (2003); Danielson et al. (2009); Boesenberg et al. (2012); Kissin et al. (2013); Ali et al. (2018); Boesenberg et al. (2018); and this study. Full data set and detailed data sources presented in Data S1.

angular olivine with geochemistry and accessory phase mineralogy.

### Olivine Geochemistry

Previous PMG subgroupings have been suggested on the basis of olivine and metal geochemistry, and the most commonly used subgroup is that defined by olivine major element composition. The PMG olivine fayalite contents indicate that there are two populations or a possible bimodal distribution. They are dominated by compositions at  $\sim\text{Fa}_{12-13}$  which include most pallasites such as Admire, Esquel, and Imilac, but with a tail in the distribution toward a small high-FeO population at

$\sim\text{Fa}_{16-18}$  defined by Rawlinna 001 (hereafter Rawlinna), Phillips County, Springwater, Sterley, and Zaisho (Buseck 1977; Scott 1977b; Shima et al. 1980; Buseck and Clark 1984; Ali et al. 2018; Fig. 2). The latter have been designated “anomalous silicate” (PMG-as; e.g., Wasson and Choi 2003; hereafter we refer to them as “high-FeO PMG-as” for consistency with both Wasson and Choi [2003] and our designation of the low-MnO subgroup). This high-FeO olivine is usually of the rounded variety (Kissin 2008, 2009). It is also associated with higher Ni contents in the metal, indicating a more oxidizing environment via loss of Fe to the silicate component (Prior 1916; Mason 1963) although there is

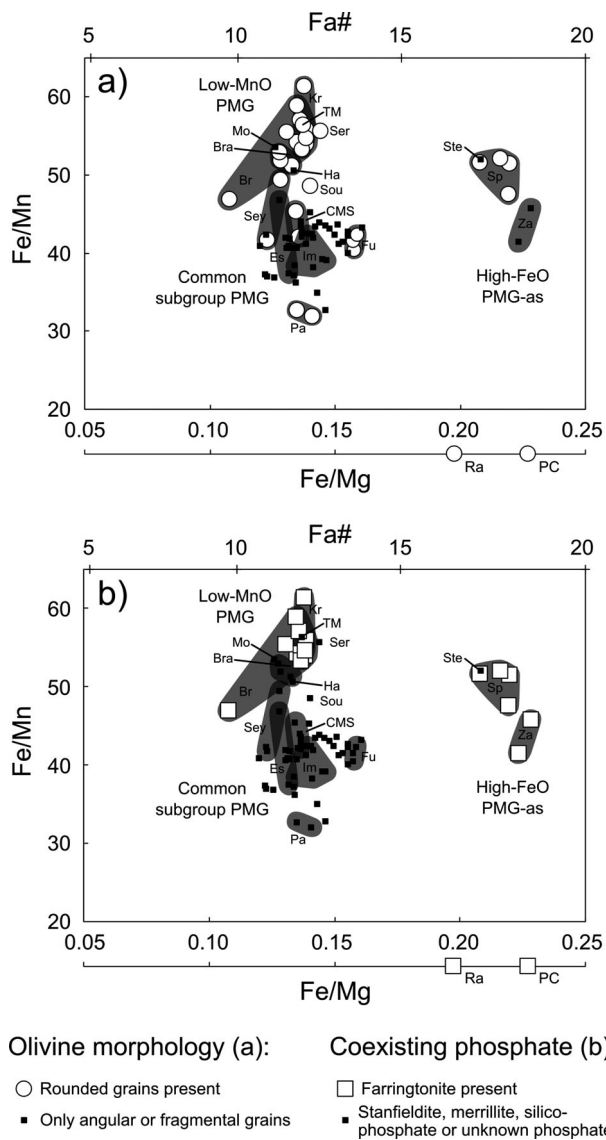


Fig. 2. Summary of PMG olivine Fe-Mg-Mn systematics (as molar Fe/Mg and Fe/Mn, including Fa#) from EMPA, (a) matched with petrographic types, and (b) with phosphate mineralogy (data sources given in supporting information). We plot all available data from the literature that are of sufficient quality, and new data from this study. Those PMG containing rounded olivine are indicated in (a) by white circles; those containing farringtonite are indicated in (b) by white squares; all other PMG are indicated by black squares. Farringtonite-bearing pallasites without information for Mn concentrations in olivine are given on a separate scale below each subfigure. Replicates of the same pallasite are indicated by gray fields. Each of the subgroups identified in this study are labeled (common subgroup PMG; low-MnO PMG, and high-FeO PMG-as). Following the method of Scott (1977a), we label selected pallasites with the following abbreviations: Brahin (Bra); Brenham (Br); Cumulus Ridge 04071 (CMS); Esquel (Es); Fukang (Fu); Hambleton (Ha); Imilac (Im); Krasnojarsk (Kr); Molong (Mo); Pavlodar (Pa); Seymchan (Sey); Springwater (Sp); Sterley (Ste); Southampton (Sou); Thiel Mountains (TM); Zaisho (Za).

considerable scatter in Ni contents due to kamacite-taenite sampling noise (Scott 1977a; Righter et al. 1990; Wasson and Choi 2003). In addition, some “anomalous metal” compositions have been identified (PMG-am in Wasson and Choi [2003], including Argonia, Brenham, Glorieta Mountain, Huckitta, Krasnojarsk, and Pavlodar; since then, Seymchan has also been attributed to the PMG-am by Van Niekerk et al. [2007]). Similar to PMG-as, there is also a strong correlation between rounded olivine textures and anomalous metal compositions (Kissin 2008, 2009). Unlike PMG-as, which identifies simple MgO-FeO exchange in olivine and complementary variation in the Fe/Ni of metal, the PMG-am designation combines several trace element peculiarities (e.g., Au-Ir systematics or Ga and Ge concentrations) and we will therefore address their geochemistry in the Trace Element Geochemistry of Olivine and Metal section.

The concentrations of MnO in PMG olivine delineate another bimodality or tail in the population to lower concentrations. In most olivine of the PMG, the concentration of MnO is ~0.30 wt% but in some, it falls to ~0.20 wt%; for PMG with olivine of ~Fa<sub>12-13</sub>, we defined these values as the common subgroup and low-MnO PMG, respectively. This variation has been reported in many studies over many years (Lovering 1957; Buseck and Goldstein 1969; Cooper 1974; Kolomeitseva 1975; Takeda et al. 1978; Smith et al. 1983; Mittlefehldt et al. 1998; Mittlefehldt 1999; Hsu 2003; Mittlefehldt and Herrin 2010; Boesenberg et al. 2012; Ali et al. 2018). Decreasing MnO content at steady Fa# results in a small number of pallasites at higher molar Fe/Mn in Fig. 2, including Brahin, which is the main focus of our study. As well as Brahin, the low-MnO PMG includes Brenham, Hambleton, Krasnojarsk, Molong, Sericho, and Thiel Mountains. Practically, one could use a cutoff value of molar Fe/Mn of ~48 at normal olivine composition of ~Fa<sub>12-13</sub> to distinguish the subgroups (olivine from the Southampton pallasite, like Seymchan, may be transitional to the two subgroups at Fe/Mn of 48.5; Kissin et al. [2013]; Table 3). Like the high-FeO PMG-as, there is a high frequency of rounded olivine in the low-MnO PMG. Because some, but not all, of these groups were also assigned to the PMG-am subgroup, Kissin (2008, 2009) suggested that there was a relationship between olivine morphology and unusual metal or olivine compositions.

We defined the remaining PMG with normal olivine compositions of ~Fa<sub>12-13</sub> and molar Fe/Mn less than ~48 as the common subgroup. They contain predominantly angular rather than rounded olivine (Fig. 2; Table 3). In Fig. 2a, we plot the Fe-Mg-Mn systematics indicate those PMG that have been reported to contain rounded olivine with large circles and others with small squares. Most PMG containing rounded olivine occur in the high-FeO

PMG-as and low-MnO subgroups. There are a few exceptions to this pattern, the most important being Pavlodar, which is anomalous in containing rounded olivine of composition  $Fa_{12.5}$  with unusually high MnO contents for the common group PMG (0.35–0.37 wt% yielding Fe/Mn of ~32; Smith et al. 1983; Boesenberg et al. 2012). Information on texture and olivine Fe-Mg-Mn systematics is lacking for some pallasites. For example, the high-FeO PMG Zaisho was first reported to contain fragmental olivine (Shima et al. 1980) and a more detailed study of a small nonrepresentative section contained abundant chromite, with only sparse olivine less than 1 mm in size (Buseck and Clark 1984). This olivine appears to be neither of the relatively large (~5 mm diameter) rounded or angular types, but fragmental grains that had undergone more extensive rounding than could be described “microscale,” as occurs in nearly all other pallasites. For a few pallasites, the Mn content of olivine has not been reported, including interesting high-FeO PMG-as such as Rawlinna and Phillips County (Fig. 2). We have compiled textural information and literature EMPA data for the Fe-Mg-Mn systematics of PMG olivine in Table 3 and in Table S2 in Data S1.

Aside from Mn, available PMG minor and trace element data are few and coverage of the various subgroups is patchy. On the scale of whole-grain olivine analyses, the large range in concentration of the refractory lithophile element Sc (0.7–2.1 ppm) in the various PMG has been used to argue for pallasite silicates as olivine restites rather than cumulates (Mittlefehldt 1999, 2005; Mittlefehldt and Rumble 2006; Mittlefehldt and Herrin 2010; Boesenberg et al. 2012). However, the large scatter in Sc contents for pallasite olivine could possibly be explained by sampling noise due to intracrystal chemical and diffusion effects, such as correlations between Al, Ti (Hsu 2003) and Sc (McKibbin et al. 2013). The concentration of Sc has a large range within olivine in Brahin (0.9–1.7 ppm; McKibbin et al. 2013), which nearly covers the whole pallasite range. Because only a small number of PMG olivine grains have been investigated in detail for in situ trace element variations, it is clear that a larger study is needed to fully understand these systematics.

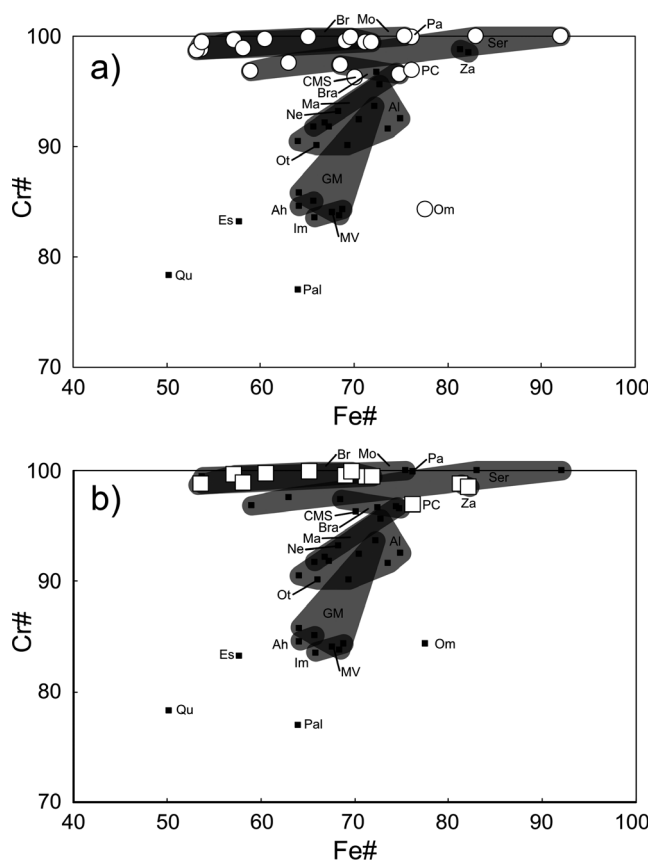
### *Phosphorus-Bearing Minerals*

The geochemistry of phosphorus in pallasites is complex but informative, and has resulted in several accessory minerals that we discuss here. Whether coherent subgroups can be identified within the PMG that gather all textural, mineralogical, and geochemical features together is an outstanding question (e.g., Boesenberg et al. 2012), and this is especially the case

for the diverse phosphate minerals and phosphoran olivine (with several wt%  $P_2O_5$ ).

There are two common phosphate minerals in most PMG and other rarer phosphate minerals. The first is merrillite, a Ca-rich anhydrous phosphate equivalent to whitlockite ( $Ca_9Na[Fe,Mg][PO_4]_7$ ), which has been reported under this name in many early pallasite studies (or approximated as  $Ca_3[PO_4]_2$ , e.g., Fuchs 1969). It is equivalent to the phosphates in many other meteorite groups such as ordinary chondrites (e.g., Hughes et al. 2008; Ward et al. 2017). The other most commonly occurring phosphate in PMG is the Ca-Mg phosphate stanfieldite (with the formula  $Ca_4[Mg,Fe]_5[PO_4]_6$  that is often approximated as  $Ca_{1.5}Mg_{1.5}[PO_4]_2$  and may exhibit a range of solid solution; Fuchs 1967). In a smaller number of PMG, the Mg-rich endmember farringtonite has been found ( $Mg_3[PO_4]_2$ ) and although it is present in fewer pallasites (eight according to Fowler-Gerace et al. 2013) it can be volumetrically abundant, at several vol% in the low-MnO PMG Krasnojarsk and the high-FeO PMG-as Springwater and possibly Zaisho (Dufresne and Roy 1961; Fuchs et al. 1973; Buseck and Holdsworth 1977; Shima et al. 1980; Buseck and Clark 1984; Fig. 2). Wahl (1965) reported farringtonite of a different color to that of Springwater in Huckitta, Marjalahti, Newport, and Pavlodar, but these occurrences do not seem to have been confirmed. The simplified Ca-Mg phosphate phase diagram presented by Ando (1958) included these three main phosphates, indicating that merrillite is a high-temperature refractory phase, that stanfieldite exhibits incongruent (peritectic) behavior and can therefore crystallize via consumption of merrillite and more Mg-rich phosphate melt, and that the eutectic lies between farringtonite and stanfieldite. Fuchs (1967, 1969) suggested that the single-phase field for stanfieldite might be larger than that reported by Ando (1958) and that the coexistence of the Mg- and Ca-bearing endmembers in the same meteorite should indicate disequilibrium. Farringtonite has only been reported in the low-MnO and high-FeO PMG-as, while stanfieldite and merrillite can occur in any subgroup. Excluding breakdown phosphates that probably formed during terrestrial weathering, there are in addition to the three common phosphates at least two occurrences of a silico-phosphate phase in Brahin and Springwater (Buseck and Holdsworth 1977) and a similar phase in Brenham reported as calcic-chladniite (Wasson et al. 1999). We have compiled phosphate mineralogy from the literature in Table S4 in Data S1, and summarize this information in Figs. 2b and 3b.

Rare earth trace element studies of phosphates in PMG found patterns typically strongly depleted in light relative to heavy rare earth elements, and generally at


**Olivine morphology (a):**

- Rounded grains present
- Only angular or fragmental grains

**Coexisting phosphate (b):**

- Farringtonite present
- Stanfieldite, merrillite, silico-phosphate or unknown phosphate

Fig. 3. Summary of PMG chromite Mg-Fe and Cr-Al systematics (as Fe# and Cr#) from EMPA, (a) matched with petrographic types, and (b) with phosphate mineralogy (data sources given in supporting information). Following the method of Scott (1977a), we label selected pallasites as in Fig. 2 with the following additional abbreviations: Ahumada (Ah); Albin (Al); Glorieta Mountain (GM); Marjalahti (Ma); Mount Vernon (MV); Newport (Ne); Omolon (Om); Otinapa (Ot); Pallasovka (Pal); Quijingue (Qu).

moderate concentrations in merrillite, but low to very low concentrations in stanfieldite and farringtonite. However, some phosphates are rich in light rare earth elements and they may have frequent strong depletions in Eu (Davis and Olsen 1991, 1996; Hsu 2003). In conjunction with the phosphate phase equilibria indicating that merrillite is a high temperature refractory phase while stanfieldite and farringtonite are present at the eutectic (Ando 1958), the trace element systematics are generally consistent with extensive fractional crystallization but with a large number of inherited, potentially xenocrystic or locally processed grains (Davis and Olsen 1991, 1996; Hsu 2003). Davis and Olsen (1991) presented trace element data for silico-

phosphate in Springwater that strongly indicate it is also of xenolithic nature, with a contrasting light rare earth element-enriched pattern. No trace element data are available for the silico-phosphate in Brahin or the calcic-chladniite in Brenham.

Phosphoran olivine with ~0.8–7.4 wt%  $P_2O_5$  has been reported in several pallasites (Buseck 1977; Buseck and Clark 1984; Wasson et al. 1999; Fowler-Gerace and Tait 2015). It is likely that continuous variation in olivine phosphorus concentration is possible, but in PMG, most normal olivines have low phosphorus contents at less than 100–200 ppm (e.g., McKibbin et al. 2013, 2016). The potentially metastable character of this mineral (Boesenber and Hewins 2010; Boesenber et al. 2012) and its presence as overgrowths on other olivine grains (Fowler-Gerace and Tait 2015) suggests its formation during rapid cooling of a silico-phosphate melt, during the termination of pallasite magmatic evolution. Phosphoran olivine has been found in the low-MnO PMG Brenham and Brahin as well as PMG-as Springwater, Zaisho, and Rawlinna, and therefore preferentially (or perhaps exclusively) occurs in pallasites that do not belong to the common subgroup PMG (Buseck 1977; Buseck and Clark 1984; Wasson et al. 1999). In Brenham, phosphoran olivine occurs in association with chromite-rich regions lacking in metal (Wasson et al. 1999).

In contrast to phosphates and phosphoran olivine, the more common phosphide mineral schreibersite ( $[Fe, Ni]_3P$ ) is present in all pallasites (table 4 in Buseck 1977). In iron and pallasite meteorites, schreibersite likely forms at lower temperature by exsolution from metal (e.g., Clark and Goldstein 1978; Yoshikawa and Matsueda 1992). In terms of trace elements, it is similar to kamacite and taenite in being a host for most siderophile elements, with possible exception of low Cu and high Ga and Mo contents (Danielson et al. 2009). Schreibersite is important in buffering oxygen in iron meteorite systems at lower temperature by its reaction relationship with phosphates (Olsen and Fuchs 1967).

### Chromite Geochemistry

Chromite is present in PMG at levels from zero to a few percent (e.g., Bunch and Keil 1971; Buseck 1977), but it can be very heterogeneously distributed and occasionally represents several tens vol% depending on sampling heterogeneity (in “massive chromite” regions in Brenham and Seymchan: Francis and Lange 1987; Wasson et al. 1999; Van Niekerk et al. 2007). The major element geochemistry of PMG chromite displays a complex distribution (Fig. 3 and Table S5 in Data S1). Chromites exhibit variable MgO-FeO exchange and a minor, variable “spinel” component via  $Al_2O_3$ - $Cr_2O_3$  exchange (i.e.,  $[Mg,Fe][Cr,Al]_2O_4$  with insignificant  $Fe^{3+}$

contents). The common subgroup PMG chromites form a noisy correlation between Fe# and Cr# (defined as molar  $100 \times \text{Fe}/[\text{Fe} + \text{Mg}]$  and  $100 \times \text{Cr}/[\text{Cr} + \text{Al}]$ , respectively) while the low-MnO pallasites have low  $\text{Al}_2\text{O}_3$  contents (chromite in Brenham and Molong has Cr# higher than 98.5, while in Brahin, it is ~97). Chromite compositions for high-FeO PMG-as have only been reported for Zaisho and Phillips County. They are also relatively poor in  $\text{Al}_2\text{O}_3$  and have the highest Fe# among PMG except for that in the common subgroup (although PMG-am) Pavlodar (Fig. 3; Table S5 in Data S1). The highest yet reported  $\text{Al}_2\text{O}_3$  contents for PMG chromite are for Pallasovka (Sadilenko et al. 2006), Quijingue (Coutinho et al. 1999; Zucolotto 2000), and Fukang (DellaGiustina et al. 2019) at Cr# ~77–78. Chromite from the Omolon pallasite, which contains rounded olivine, appears as an outlier to all other pallasites in Fig. 3, perhaps because only compositional data for small chromite inclusions are available (Sharygin et al. 2006).

There are therefore correlations between several characteristics in PMG that have been masked by disparate studies on limited samples, but are clear from a synthesis of the literature (Table 3; Figs. 2 and 3; Data S1). Anomalous olivine geochemistry, either as high-FeO PMG-as or low MnO PMG, is preferentially associated with rounded olivine morphologies, accessory or abundant farringtonite, rare silico-phosphate (or calcic-chladniite), and phosphoran olivine. As well as predominantly rounded olivine morphologies, the low-MnO PMG contain low-Al chromite, while the chromite in common subgroup PMG exhibits a correlation between Mg and Al contents.

### PMG Textures and Candidate Liquids to Drive Rounding of Olivine

The driving force for rounding of olivine in pallasites is minimization of interfacial energy between olivine crystals or crystal fragments and the matrix (Scott 1977b; Ohtani 1983), approximated by a reduction in the olivine surface area (Scott 2017). Olivine rounding is independent of grain growth and the latter may be suppressed if grains are isolated from each other, because olivine chemical components are highly insoluble in metal. In this case, the reduction of interfacial energy between grains is achieved at constant grain volume and only through changes in shape (Saiki et al. 2003). However, most rounded olivine in pallasites probably forms part of an interconnected network, while angular olivines exhibit their morphologies precisely because they are in contact with other olivine grains or were in such an arrangement shortly before being separated by intruding metal (Buseck 1977; Spinsby et al. 2008). The growth of large grains

proceeds at the expense of small grains, and can occur via Ostwald ripening when a matrix is present (Lifshitz and Slyozov 1961; Wagner 1961) or as “normal” grain growth in a monomineralic system (Atkinson 1988). Both mechanisms are applicable to pallasites, and higher growth rates prevail at high sulfur contents (Gaetani and Grove 1999; Solferino et al. 2015).

With the clear case of large (frequently ~4–5 mm and up to ~6 mm diameter) rounded olivine in the low-MnO Brahin pallasite and some crystals with partially angular features, in addition to already well-documented fragmental olivine (Fig. 1), it is worth re-evaluating grain growth and rounding in pallasites and potential correspondence among texture, mineralogy, and geochemistry. The presence of rounded or angular olivine grains seems to be partly a function of how close set the olivine grains are to one another, and whether they share mutual boundaries, as observed here for Brahin but also relevant to many other pallasites such as Brenham and Seymchan (the latter containing angular, rounded, and fragmental olivine; Van Niekerk et al. 2007; Kichanov et al. 2018). One particular difficulty in understanding pallasite petrogenesis has been in finding coherent relationships between these characteristics, including the occurrence or absence of accessory phases such as phosphate minerals and phosphoran olivine. The latter is a conspicuous phase which, among meteorites, is almost unique to pallasites (Wasson et al. 1999; Boesenberg and Hewins 2010; Boesenberg et al. 2012; Fowler-Gerace and Tait 2015) with only a few rare occurrences in other types such as Martian meteorites (Goodrich 2003), carbonaceous chondrites (Wang et al. 2006), and IIE iron meteorites (Van Roosbroek et al. 2015, 2017). Phosphoran olivine with  $\text{P}_2\text{O}_5$  at the level of several weight percent is present in low-MnO PMG Brahin and Brenham, and in high-FeO PMG-as Rawlinna, Springwater, and Zaisho (Buseck 1977; Scott 1977b; Buseck and Clark 1984; Wasson et al. 1999; Table 3). It seems to be more common in high-FeO PMG-as Springwater (Fowler-Gerace and Tait 2015) and Zaisho (Buseck and Clark 1984) but is absent in common subgroup PMG, indicating that there is no simple relationship to fayalite content (Table 3). Previously, in the absence of known rounded olivine in Brahin, it was concluded by Boesenberg et al. (2012) that “there is no obvious correlation between phosphoran olivine and either olivine composition or texture.” Now, with rounded olivine in Brahin, it seems that phosphoran olivine is confined to low-MnO and high-FeO olivine subgroups, which also preferentially exhibit rounded olivine. It is not known from the common PMG subgroup, which is dominated by angular olivine, for example, Admire, Esquel, and Imilac (Table 3).

Phosphoran olivine is potentially metastable, being intermediate in composition between normal, stoichiometric olivine (containing phosphorus at the level of just a few tens or hundreds ppm) and true phosphate minerals in pallasites (Boesenberg et al. 2012). This suggests that the  $P_2O_5$  component in pallasites should be considered as an incompatible component in a magmatic system, in which  $P_2O_5$  is hosted in a melt which crystallizes to olivine and one or more phosphates, or to phosphoran olivine as a quench product. Late crystallization of phosphoran olivine, or the more common assemblage of normal, low- $P_2O_5$  olivine with one or more phosphate minerals, indicates that the partially molten assemblage of metal, olivine, chromite, troilite, and phosphate, wetted by interstitial immiscible metal-sulfide-phosphide and silico-phosphate liquids, underwent final cooling from magmatic temperatures. This effectively terminated the evolution of the melt (Fowler-Gerace and Tait 2015). The presence of phosphoran olivine overgrowths on round olivines is initially encouraging for an interstitial silico-phosphate melt to promote rounding, with a “phosphorus-bearing silicate melt” having been suggested by Boesenberg et al. (2012). Phosphoran olivine is common in PMG-as Springwater and Zaisho and is also present in Rawlinna (Buseck 1977; Buseck and Clark 1984). However, it poses problems because a silicate melt wetting olivine surfaces should enhance the euhedral form of olivine grains, resulting in conventional igneous textures. This is illustrated in Springwater by common phosphoran olivine overgrowths containing internal serrated oscillatory zoning crystallized epitaxially over normal olivine, with later growth layers having smoother and more undulating morphologies, finally terminating against metal or farringtonite (Fowler-Gerace and Tait 2015). Additionally, phosphoran olivine is rare in the low-MnO PMG having only been observed in Brahin and Brenham, and therefore, a silico-phosphate melt was unlikely to have been present in sufficient amounts to drive rounding in such pallasites (Buseck 1977; Buseck and Clark 1984; Wasson et al. 1999). The common occurrence of phosphoran olivine in massive chromite regions of Brenham, but not other parts of the meteorite, is a good indication that phosphoran olivine and rounding are not directly related (Wasson et al. 1999). Phosphoran olivine has not yet been found in Krasnojarsk, Hambleton, Molong, Phillips County, Sericho, Seymchan, Sterley, or Thiel Mountains although it might be expected (Krasnojarsk has instead been reported to contain locally abundant farringtonite). Neither has phosphoran olivine been found in the anomalous PMG-am Pavlodar, which contains conspicuously rounded olivine with a higher

MnO content. The high Ir content of the metal in this pallasite suggests a primitive composition that might therefore have had low P contents (Wasson and Choi 2003). It seems likely that the presence of phosphoran olivine in pallasites and former presence of silico-phosphate melt are simply correlated with rounded olivine textures, rather than one being the cause of the other.

Better candidates for the melts that enable rounding of olivine are perhaps found in the nonsilicate constituents of pallasites in which an olivine component is highly insoluble, such as liquid metal-sulfide or -phosphide. The rate of rounding and grain growth is strongly enhanced by the presence of a liquid, and in the absence of a liquid, it may only be possible to drive rounding on a microscale over geological timescales (Ohtani 1983). In a sulfide- and phosphide-free system at high temperatures (1400 °C; although still subsolidus and under conditions preventing grain growth), olivine-metal mixtures were readily able to generate microscale rounding (Saiki et al. 2003). However, these conditions were only marginally able to achieve rounding rates consistent with rounding larger olivine with diameters of 500  $\mu\text{m}$  over  $\sim 2$  Myr and much longer timescales for larger olivine grains. It is therefore plausible that microscale rounding of angular or fragmental olivine records the trapping and isolation of these grains in solid metal shortly after olivine separation or fragmentation, shortly after nearly complete crystallization of the metallic groundmass (Scott 2017). This would occur as temperature dropped to near the solidus ( $\sim 950$  °C; Raghavan 2004; Starykh and Sineva 2012). The experiments of Saiki et al. (2003) also imply that sulfide and phosphide in the liquid play a critical role in enhancing diffusion rates. Solferino et al. (2015) confirmed the effect of liquid metal-sulfide in enhancing rates of both grain growth and rounding. Although they could not unambiguously identify the grain growth mechanism likely for pallasite olivine (probably a mixture of Ostwald ripening and grain-boundary migration) and had higher sulfur contents in their experiments than in natural pallasites, the obtained growth rates are the most applicable to natural systems. At temperatures of  $\sim 1300$  °C only relatively short timescales of  $\sim 0.1$  Myr are required to achieve the typical maximum pallasite grain size of  $\sim 10$  mm (fig. 7a in Solferino et al. 2015). This timescale would probably be slightly longer at lower sulfide content and lower temperatures nearer the solidus, as long as the assemblage contained sufficient melt ( $\sim 950$  °C; Raghavan 2004; Starykh and Sineva 2012).

Considering the ubiquity of the phosphide mineral schreibersite in pallasites, another possible liquid responsible for rounding of olivine might be a phosphorus-rich metallic liquid. Immiscibility between Fe-sulfide and Fe-phosphide has long been considered for meteorites (Kracher et al. 1977; Ulf-Møller 1998a) guided by early

studies of Fe-S-P systems (Schürmann and Schäfer 1968; Schürmann and Neubert 1980; Raghavan 1988). However, some petrographic observations of iron meteorites as well as refinements to the phase diagram suggest that schreibersite would usually form only by exsolution under subsolidus conditions and that immiscibility might be difficult to achieve (Clark and Goldstein 1978; Yoshikawa and Matsueda 1992; Chabot and Drake 2000). Practically, any rounding or grain growth effects due to a heterogeneously distributed P-rich liquid metal might be difficult to distinguish from liquid metal-sulfide. Our inference of domains in Brahin containing only a single accessory mineral over the ~cm scale (Fig. 1b) suggests that sulfide-phosphide immiscibility indeed did occur in the Brahin region of pallasites and could be responsible for some rounding of olivine. Similar observations have been reported for the sulfide-rich low-MnO pallasite Hambleton (Johnson et al. 2006a, 2006b) as well as the common subgroup pallasite CMS 04071 in which some rounded olivine has been reported (Danielson et al. 2009; Table 3). For Brahin, liquid Fe-sulfide or Fe-phosphide may both be responsible for the olivine rounding, but in the section that we studied, large (frequently ~4–5 mm diameter and some larger) rounded olivine does not seem to be preferentially associated with either sulfide or phosphide, but rather with chromite (Fig. 1a).

The heterogeneous distribution of accessory chromite and phosphate minerals in most pallasites indicates that these phases are not responsible for rounding, consistent with expectations for solid-state transformations (Ohtani 1983). These phases are present at abundances of only a few percent at most (e.g., farringtonite in Springwater and Krasnojarsk; Buseck 1977) and although chromite and rounded olivine are associated in Brahin in Fig. 1, they are usually heterogeneously distributed with no correspondence between olivine morphology and local mineralogy (e.g., massive chromite in Brenham and Seymchan; Francis and Lange 1987; Wasson et al. 1999; Van Niekerk et al. 2007). The continuous textures in pallasites containing rounded olivine are more consistent with the liquid responsible for rounding being an interconnected, small degree Fe-S melt saturated in crystalline metal, troilite, and chromite (with possible immiscibility generating an additional Fe-P melt) that migrated out of the pallasite assemblages at a late stage in its crystallization and rounding history, as also concluded from the low abundance of sulfide in pallasites (Buseck 1977; Ulff-Møller et al. 1998).

### The Distribution of Mn in PMG Olivine and Origin of Low-Degree Melts

The common PMG contain angular olivine and polycrystalline olivine masses as their primary

morphologies (Buseck 1977; Scott 1977b). Boesenberg et al. (2012) suggested that common PMG formed by very thorough extraction of silicate melt from the solid, refractory olivine host, resulting in the production of triple junction boundaries between adjacent olivine grains, and ultimately large masses of olivine. The occurrence of frequently disaggregated olivine masses intruded by metal indicates that common PMG are effectively simple mechanical mixtures of olivine and metal. This olivine may be typical of the “middle mantle” of the pallasite parent body intruded by variably evolved metal (Boesenberg et al. 2012) over various depths (Yang et al. 2010), although magmatic temperatures are far above kamacite–taenite exsolution temperatures and this may mask a long interval in pallasite history (Fowler-Gerace and Tait 2015). The common PMG, like most pallasites, contain remarkably little sulfide (e.g., Ulff-Møller et al. 1998) and no indication of a silico-phosphate melt (lacking phosphoran olivine and farringtonite; Table 3). Rather, their potentially xenocrystic merrillite and stanfieldite (Davis and Olsen 1991, 1996; Hsu 2003) in combination with angular or fragmental textures suggest that the common PMG pallasites do not represent quiescent core–mantle boundaries (in agreement with Yang et al. 2010). Rather, these mechanical mixtures cooled through the solidus over rapid timescales or rapidly expelled their final liquids in order to isolate olivine and prevent rounding (Solferino et al. 2015; Scott 2017).

Unlike the common PMG, pallasites of the low-MnO or high-FeO subgroups contain accessory reaction products including farringtonite and phosphoran olivine, and do not seem to be simple mechanical mixtures of core and mantle materials. Some PMG have been reported to contain only stanfieldite (e.g., Molong and Thiel Mountains in the low-MnO subgroup, and Newport in the common subgroup; Buseck and Holdsworth 1977; Davis and Olsen 1996), while Brahin contains stanfieldite, silico-phosphate, and phosphoran olivine (Sonzogni et al. 2009). However, the more diagnostic minerals farringtonite or merrillite have not yet been observed in these pallasites. We anticipate that further phosphate reports in these and other PMG will follow the trend that we have established.

The common PMG and the low-MnO PMG, despite their dissimilar textures, share the same major element composition at ~Fa<sub>12</sub> but differing contents of MnO (Mittlefehldt 1999; Hsu 2003; Boesenberg et al. 2012). The rounded olivine in the latter seems to indicate that Mn has some affinity for the liquid responsible for rounding. This liquid was previously suggested to be liquid metal-sulfide (e.g., Ohtani 1983; Solferino et al. 2015) or a silico-phosphate melt, due to

the occurrence of phosphoran olivine and the Mg-phosphate farringtonite in these pallasites (Boesenberg et al. 2012). The presence of a late, interstitial, Mn-rich melt in pallasites is indicated by Mn-rich rims on olivine in some pallasites. Of the common subgroup PMG, there is slight enrichment of Mn in olivine from Albin (Hsu 2003) but not in others such as Esquel and Imilac (Miyamoto 1997). One report of Mn zoning in Springwater olivine (Zhou and Steele 1993) stands in contrast to other studies (Leitch et al. 1979; Fowler-Gerace and Tait 2015). However, among low-MnO pallasites, enrichment of Mn in olivine rims is quite clear, indicated by vertical trends in plots of olivine Fe/Mg versus Fe/Mn (fig. 2a in Boesenberg et al. 2012) and in line profiles approaching olivine margins (McKibbin et al. 2016). The higher MnO in rims of olivine from low-MnO PMG indicates potential late diffusion of Mn into olivine, or late overgrowths. In either case, it implies two stages of equilibration or crystallization of olivine, the first to establish homogeneous interiors (by comparison with common PMG, in the presence of a preferred host for Mn) and the second in which the Mn was redistributed into the olivine rims under different boundary conditions. This model stands in contrast to those in which Mn is considered to be unmodified by repartitioning between olivine and metal or sulfide (e.g., Mittlefehldt 1999). In a series of olivine-metal equilibration and diffusion experiments, Donohue et al. (2018) found very rapid diffusion of Mn in olivine under pallasitic conditions. They inferred that most trace elements in PMG equilibrated across olivine crystals coexisting with metal at relatively high temperatures, in the range ~1300 and ~1550 °C for Mn in Glorieta Mountain and Albin, and at 1200 °C or higher for Cr in most pallasites (the latter approaching Al-in-olivine temperatures of ~1000–1290 °C from McKibbin et al. [2013] and Prissel et al. [2017]). We conclude that if PMG with normal levels of MnO sample a general starting material for subsequent evolution into low-MnO PMG or other types, then any evidence for early losses or gains of Mn has long since been erased. In the next section, we will use the available literature data to evaluate the role of accessory phases and interstitial melts in controlling the geochemistry of Mn in the PMG environment.

#### Accessory Phase Controls on Mn and the Petrogenesis of Low-MnO PMG

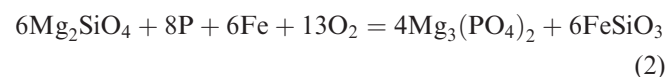
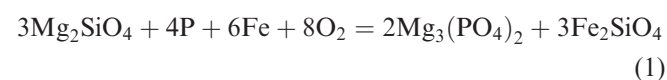
In order to understand the Fe-Mg-Mn systematics of pallasites, the various hosts for Mn, and ultimately the potential sinks for Mn that might be responsible for the low-MnO PMG, we review here the petrogenesis of

those accessory phases (or their sources) that have potential to change the mass balance. These include the various phosphate minerals or their precursor phosphate melt, troilite or its precursor sulfide melt, and chromite.

#### *Phosphate Minerals and (Silico-)Phosphate Melt*

The various phosphate minerals in PMG are minor hosts for Mn at variable levels. In the low-MnO pallasites, the least common but potentially voluminous Mg-phosphate farringtonite has been found in Krasnojarsk at an abundance of ~1 vol%, while a single occurrence has been reported for in Brenham (Buseck 1977; Wasson et al. 1999). Farringtonite seems to be more abundant in the high-FeO PMG-as, especially in Springwater (~4%) and is also present in other members of that group (Buseck 1977; Buseck and Holdsworth 1977; Buseck and Clark 1984; Fig. 2b). The highly lithophile character of Mg is strongly indicative of farringtonite being produced in large amounts by reaction of olivine or primitive silicate melt with a reservoir of phosphorus and perhaps oxygen. Oxidation of phosphorus that was originally present in the metallic liquid has been suggested in many previous studies, and it was likely present in the pallasitic metallic liquid at the level of ~2–4% (e.g., Davis 1982). Similar to the kinetics of rounding and grain growth of olivine, these reactions may have been more likely to occur at higher temperatures in a partially molten state involving phosphorus in liquid Fe-Ni metal coexisting with olivine or ultramafic silicate melt, rather than in the subsolidus state involving phosphorus in metal or schreibersite (as suggested by Davis and Olsen 1991).

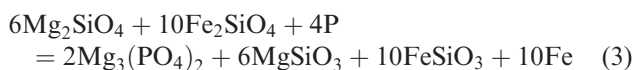
The production of significant farringtonite could proceed according to:



after Olsen and Fredriksson (1966) and Fuchs (1967) (Equation 1); and modified from Davis and Olsen (1991) (Equation 2). These reactions generate either fayalite or ferrosilite, and the former would be qualitatively consistent with the production of high-FeO PMG-as such as Springwater by conversion of some of the forsteritic component of common PMG olivine to a fayalitic component (although this would not explain

higher Ni content in the metal of these pallasites). For Krasnojarsk, the production of 1 vol% farringtonite by this mechanism would probably not go unnoticed in a corresponding enrichment in the fayalite component of olivine, but by comparison with other low-MnO PMG such as Brenham, this does not seem to have occurred. We note, however, that the total area of Krasnojarsk studied in Buseck (1977) is only 38 cm<sup>2</sup> compared to 475 cm<sup>2</sup> for Brenham and 376 cm<sup>2</sup> for Springwater. The high abundance of farringtonite and lack of other phosphates in Krasnojarsk might indicate unrepresentative sampling, and a lower modal proportion of farringtonite production by Equation 1 might not increase the fayalite content of olivine in this pallasite by very much. By contrast, the latter reaction (Equation 2) would require the presence of a silicate melt to carry away the excess pyroxenite component.

Alternately,



was suggested by Kracher (1983) but results in even more abundant pyroxene for a given amount of farringtonite. The absence of large pyroxene masses in these pallasites suggests that Equation 3 was not important for the production of farringtonite. In support of a pyroxene-free production of farringtonite, Brunet and Laporte (1998) produced synthetic analogs to pallasites (in a Ni- and S-free system at moderate pressure) containing farringtonitic melts coexisting with olivine and metallic melt, with stoichiometry achieved via modification of the olivine composition (presumably via Equation 1). While loss of a pyroxenitic silicate melt is also an option, the correspondence between rounded olivine, anomalous (low-MnO or high-FeO) olivine geochemistry, and the presence of farringtonite and the occasional closely related phosphoran olivine, all suggest that a relatively simple magmatic environment was responsible for the petrogenesis of such pallasites.

The MnO contents of farringtonite as obtained by EMPA are available for Krasnojarsk, Springwater, Zaisho, and Rawlinna (Fuchs et al. 1973; Buseck and Holdsworth 1977; Shima et al. 1980; Buseck and Clark 1984; Davis and Olsen 1991). For this data set, Krasnojarsk farringtonite has the lowest MnO and FeO content (0.13 and 2.7 wt%; Fuchs et al. 1973). Farringtonite in Zaisho has the highest reported MnO (0.25 wt%; Shima et al. 1980) while that in Rawlinna has the highest FeO (5.67–5.78 wt%; Buseck and Holdsworth 1977); that is, the FeO content of farringtonite does not correlate with that of olivine. Farringtonite grains in Zaisho are well resolved from

each other by EMPA, with MnO and FeO contents spanning the entire reported range for this mineral in PMG (Buseck and Clark 1984). Farringtonite is therefore only a minor host for Mn in the low-MnO PMG such as Krasnojarsk (where its abundance may have been overestimated due to possible heterogeneity) and of even lesser importance in others such as Brenham (where only one occurrence has been reported). It is, however, more important for the high-FeO PMG-as, but does not seem to be well equilibrated either at the scale of a polished section, or within each region responsible for production of the various PMG subgroups.

The MnO contents of the Mg-Ca-phosphate stanfieldite in Springwater and Rawlinna are higher than their coexisting farringtonite grains at 0.45–0.66 and 0.25–0.32 wt%, respectively, although they may also not be at equilibrium due to the coexistence of more than two phosphate minerals in the same meteorites (Buseck and Holdsworth 1977; Davis and Olsen 1991). Unfortunately, stanfieldite has not been observed in Krasnojarsk, and MnO was not reported for this mineral in Zaisho (Buseck and Clark 1984). The MnO contents of stanfieldite grains in other PMG are similar and typically ~0.3–0.4 wt% (Buseck and Holdsworth 1977) although with one higher report for Omolon (0.35–0.55 wt%; Sharygin et al. 2006). Stanfieldite is therefore another minor host for Mn, but its lower volumetric abundance in most pallasites (usually much less than 1 vol%; Buseck 1977) suggests that it is not responsible for the depletion of Mn in the olivine of low-MnO PMG. Trace element coverage for stanfieldite is poor, but the possibility that some may be xenocrystic in the same way as merrillite also needs to be further investigated (Davis and Olsen 1991; Hsu 2003).

Finally, of the three main phosphate minerals, the refractory calcic endmember merrillite seems to have the least potential to be an important host for Mn, with levels near or below EMPA detection limits (~0.05 wt% in Buseck and Holdsworth 1977), and with the added complication that such phosphates are likely to be nonequilibrium phases or even xenocrystic. A lack of complete equilibrium is indicated by the presence of farringtonite, as in Springwater and Rawlinna (Ando 1958). The high rare earth element contents of merrillite also indicate a petrogenesis involving a trace element-rich melt (Davis and Olsen 1991; Hsu 2003; Boesenberg et al. 2012). Some of the stanfieldite grains also exhibit such xenocrystic trace element patterns, likely excluding them as an important host for Mn in the low-MnO PMG (Davis and Olsen 1991; Hsu 2003). The occurrence of every pallasite phosphate in one or another low-MnO PMG (merrillite, stanfieldite,

farringtonite, and silico-phosphate including potentially distinct calcic-chladniite) indicates that phosphates have not reacted to equilibrium across the entire low-MnO PMG region (Fig. 2b). We therefore conclude that phosphate minerals are probably not the main controlling factors in the Fe-Mg-Mn systematics of PMG and especially those of the low-MnO PMG.

Although phosphate minerals themselves are unlikely to be responsible, a silicate, phosphate, or silico-phosphate melt should also be briefly considered. An olivine/silicate melt partition coefficient for Mn of approximately unity prevails at conditions relevant to pallasites and is not sensitive to the pressures (fugacities) of oxygen ( $fO_2$ ) or sulfur ( $fS_2$ ; e.g., fig. 6 in Gaetani and Grove 1997). The MnO content of phosphoran olivine in low-MnO and high-FeO PMG-subgroups may serve as a proxy for a silico-phosphate melt. It is, however, very similar to that of coexisting olivine and Mg-bearing phosphates farringtonite and stanfieldite (e.g., 0.26–0.52 wt%: Buseck 1977; Buseck and Clark 1984; Fowler-Gerace and Tait 2015). Extraction of a voluminous silico-phosphate melt therefore does not seem to be an obvious sink for Mn. We will consider a different case of melt escape below.

#### *Troilite and Sulfide Melt*

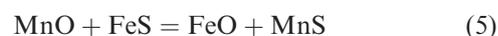
Troilite (FeS) is present in all pallasites at levels of around one or a few percent (e.g., Buseck 1977). It is clear that the present abundance of troilite in pallasites is lower than expected from the geochemistry of the metallic phases, and that liquid sulfide must have somehow been lost (Ulff-Møller et al. 1998). However, the partially chalcophile character of Mn might still be recorded in troilite Mn concentrations or could be inferred from previous work on such systems. There are not many data available for Mn in pallasite troilite but where given they are quite low compared to olivine. Danielson et al. (2009) reported 0.025 wt% Mn in troilite from CMS 04071 using EMPA (along with Cr contents of 0.09 wt%), while Zucchini et al. (2018) report a single analysis of sulfide from Mineo with 0.01 and 0.07 wt% Mn and Cr (their table A3). Such levels are in general agreement with early determinations on separated bulk troilite from Brenham and Springwater, both yielding 0.032 wt% for Mn as well as 0.14 and 0.09 wt%, respectively, for Cr (Lovering 1957), consistent with in situ methods assuming very slight contamination of the bulk troilite sample by another phase. Similar levels of 0.017–0.053 wt% were reported for troilite from the IIIAB iron Cape York (Jochum et al. 1975), which is geochemically very similar to pallasitic metal. Troilite therefore seems to be a poor host for Mn. Considering its low volumetric abundance, it is probably less significant for the subsolidus mass

balance of Mn in the low-MnO PMG than most other accessory phases.

Although troilite itself may not host much Mn, the Fe-Ni-sulfide melt from which it crystallized can host higher levels. A number of experimental studies are relevant to the partitioning and Mn budget of pallasites, especially those at low or only moderate pressures and low  $fO_2$  and water contents. In Fe-bearing systems comprising silicate and sulfide melts, the partitioning of partially chalcophile divalent trace elements such as Mn between silicate and sulfide is controlled by reactions such as:



and



with sulfide-silicate partition coefficients a function of  $fS_2^{0.5}/fO_2^{0.5}$  and not a strong function of pressure (Gaetani and Grove 1997; Li and Audétat 2012; Kiseeva and Wood 2013). At conditions relevant for pallasites, Mn can exhibit partially chalcophile behavior and partitions into sulfide melt at sufficiently high  $fS_2/fO_2$ . In the experiments of Drake et al. (1989) in which sulfide was present but  $fS_2$  was not controlled, Mn exhibited very slightly chalcophile around the IW buffer, with a  $D$  value of  $\sim 0.1$  increasing to  $\sim 1$  as  $fO_2$  was lowered over the next one to two orders of magnitude. However, these experiments were probably conducted under quite low effective  $fS_2$ . The experiments of Gaetani and Grove (1997) were conducted under controlled  $fO_2$  and  $fS_2$  and also crystallized olivine and chromite. Here, Mn was found to be partially chalcophile, but only at quite low FeO contents in the silicate melt (FeO  $\sim 3$ –4 wt% and  $D$  values for Mn around unity at  $\log fS_2^{0.5} - \log fO_2^{0.5} = 4.5$ , corresponding to very slightly below the IW buffer). This outcome was supported by moderate pressure experiments by Kiseeva and Wood (2013) in which  $D$  for Mn of  $\sim 1$  was obtained at FeO contents of  $\sim 5.0$  wt% in silicate melt, that is, still quite low compared to pallasite olivine or likely silicate melts (the partitioning of FeO for olivine-silicate assemblages is close to unity in  $Fe^{2+}$ -dominated basaltic systems, e.g., Gaetani and Grove 1997; Putirka 2005, 2016; Toplis 2005; Mysen 2007; Matzen et al. 2011). This indicates that  $D$  values for Mn were very unlikely to be near to or higher than unity in the PMG environment, and only partially chalcophile behavior is expected.

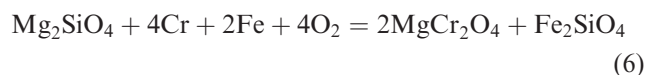
Nevertheless, the potentially strong influence of sulfide on Mn distribution in olivine-sulfide mixtures is supported by other types of experiments originally

intended to assess rates of olivine rounding and grain growth, but which also yielded hints as to the fate of Mn in such systems. Such experiments have been conducted on olivine-sulfide assemblages in the absence of silicate melt, with rather high modal contents of sulfide (~10–30 vol%). Gaetani and Grove (1999) conducted olivine-sulfide experiments at similar conditions to those presented in their earlier study on sulfide-silicate melt partitioning (1350 °C and various  $fO_2$  and  $fS_2$  in Gaetani and Grove 1997). They reported low MnO contents in olivine indicating variable degrees of extraction, dropping from 0.14 wt% in their starting San Carlos to 0.05–0.13 wt% in their product olivine. The complete Mn inventory was not fully accounted for in the recombined sulfide melt composition obtained from sulfide quench products and may be hosted in small Mn-rich phases. Similarly, the olivine reported in Solferino et al. (2015) lost about half of its Mn inventory, dropping from 0.23 wt% in their starting San Carlos to levels of typically 0.09–0.12 wt% in the products. These experiments indicate that in the absence of chromite and silicate melt, high modal sulfide contents might be able to extract significant Mn from olivine, which presumably crystallizes as heterogeneously distributed alabandite (MnS) or could be taken up by chromite in natural systems.

### Chromite

Chromite is a very common accessory phase in PMG but is heterogeneously distributed (mostly ~1 but locally up to 30 vol% in section depending on sampling heterogeneity; Buseck 1977; Wasson et al. 1999). The diverse major element chemistry of chromite enables it to track two processes in pallasitic environments. The  $Al_2O_3$  content records the former presence of silicates, especially plagioclase or a basaltic component, and chromites with variable alumina contents are found in common subgroup PMG that also contain predominantly angular olivine. In low-MnO PMG and high-FeO PMG-as that also contain predominantly rounded olivine, alumina contents are low or very low, strongly suggesting an origin that does not involve, or has much less to do with, an Al-bearing silicate melt. While Cr-Al systematics are preserved due to their slow interdiffusion in chromite (Suzuki et al. 2008), this mineral simultaneously tracks Mg-Fe exchange with olivine on shorter timescales due to relatively fast interdiffusion of these elements in both phases (Van Orman and Crispin 2010; Vogt et al. 2015). During decreasing temperature, the Mg# of chromite falls and that of olivine rises, with zoning especially obvious near rims or the interface between both phases (Wasson et al. 1999). The production of voluminous Mg-bearing and low-Al chromite, by analogy with Equation 1 for

phosphates, could proceed according to a simple reaction such as:



and the remaining pure chromite component  $FeCr_2O_4$  could crystallize directly from the metallic melt. As for the P- $P_2O_5$  reaction occurring in the presence of xenocrystic phosphates, in the common subgroup PMG, this occurred for Cr in the continuous presence of chromite indicated by some chromites with significant  $Al_2O_3$  contents (Ulff-Møller 1998b; Wasson et al. 1999). In this scenario, chromite may be a refractory, restitic phase or contain inherited cores. Other metal-bearing meteorites provide clear evidence for metallic melts evolving toward or finally becoming buffered by P- $P_2O_5$  and Cr- $Cr_2O_3$  redox reactions. These include troilite nodules in IIIAB iron meteorites associated with schreibersite, chromite, and various phosphate minerals (Olsen et al. 1999) and  $P_2O_5$ - and  $Cr_2O_3$ -rich rims on silicate inclusions in the IIE iron Netschaëvo, which crystallized phosphoran olivine and chromite (Van Roosbroek et al. 2015, 2017).

For olivine-chromite Mg-Fe exchange, Wasson et al. (1999) calculated quite low temperatures of 600–800 °C, that is, far subsolidus and indicating extensive re-equilibration between these minerals during cooling. Geothermometry by Al-in-olivine coexisting with spinel is more likely to preserve crystallization temperatures (Wan et al. 2008; Coogan et al. 2014). Quite low Al contents are present in pallasite olivine, with lower contents for a given chromite composition indicating lower temperatures. McKibbin et al. (2013) used laser ablation inductively coupled plasma mass spectrometry to find 15–30 ppm Al in Brenham and 3–33 ppm in Brahin; similar values of 10–50 ppm were found by Prissel et al. (2017) for Brahin using EMPA. These correspond to temperatures of ~1000 to 1290 °C (Prissel et al. 2017). However, the lack of much correspondence between Al distributions in olivine and the olivine morphologies also indicates that these distributions do not necessarily relate to the current petrographic arrangement, and that cores may not have been well equilibrated (McKibbin et al. 2013). Decreasing Al contents at olivine margins indicate either late overgrowths at lower temperature or diffusive modification of olivine, consistent with prolonged grain rounding in the presence of a liquid and in equilibrium with chromite (e.g., Solferino et al. 2015). The lower Al-in-olivine temperatures of ~1000 °C are broadly consistent with residence in a Fe-Ni-S melt (eutectic ~950 °C; Raghavan 2004; Starykh and Sineva 2012)

although perhaps not with lower temperatures associated with more complex Ni- and P-bearing melts (Ni-P eutectic at 850–875 °C; Doan and Goldstein 1970).

Chromite in PMG is an important host for Mn, of which the concentrations are imperfectly correlated with Fe#. Most have MnO concentrations in the range 0.51–0.84 wt%, but some lower MnO concentrations are found in the cores of chromite in the low-MnO PMG Brenham and Molong (down to 0.30 wt%; Wasson et al. 1999) and a few higher values were reported from some of the common subgroup PMG (1.13, 1.02, and 0.93 wt% in Glorieta Mountain, Marjahlati, and Pavlodar, respectively). Higher Mn combined with lower Al in the rims of Brenham chromites indicates that although olivine-chromite re-equilibration may well occur, the growth of new chromite in the presence of decreasing amounts of silicate melt is also important (Wasson et al. 1999). However, diffusive redistribution of Mn in chromite is very likely to have occurred, because of the likely similar diffusion rates to Fe in chromite (Van Orman and Crispin 2010). Therefore, even though Mn and Al zoning might correlate, they are almost certainly controlled by different diffusion processes.

The IIIAB iron meteorites are geochemically very similar to pallasitic metal (if not in fact genetically related) and serve as a test of the role of olivine in pallasitic systems. By contrast with pallasites, in the absence of silicate phases and lacking a source of Mg and Al, the chromite in IIIAB irons is almost pure chromite ( $\text{FeCr}_2\text{O}_4$ ) with a significant Mn content that is presumably derived from the metal-sulfide melt (~0.5–2 wt% MnO; Olsen et al. 1999). Chromite therefore has a high capacity to trace the Mn concentration of the metal-sulfide, but in pallasites, it is also likely to re-equilibrate with olivine during slow cooling. By analogy with Mg-Fe exchange, the Mn content of chromite should increase with decreasing temperature and the present MnO contents in pallasite chromite are therefore likely to be upper limits for magmatic temperatures. In any case, some combination of metal-sulfide melt and chromite are likely to be responsible for the depletion of Mn in the low-MnO PMG subgroup, which also contains rounded olivine indicative of a considerable residence time in Fe-Ni-S melt.

### Modal Mineralogy of Pallasites and Use of Mn as a Tracer of Melt Escape

The partial compatibility of Mn in liquid sulfide (and in chromite, which crystallizes from this liquid) might be reflected in the modal mineralogy of PMG and could potentially be used to track the depletion of sulfide in the pallasite parent body. Although the coarse

grain size of pallasites adds sampling noise, most determinations of modal mineralogy have found less than 5 vol% troilite and less than 2 vol% chromite (Buseck 1977). On the basis of troilite/olivine and chromite/olivine ratios, a number of PMG stand out at high values for one or both, while most lie near the origin reflecting high olivine contents (Fig. 4; in these ratios, we use troilite as a tracer of sulfide and olivine rather than Fe-Ni metal, because Mn is not hosted in metal). Regions of massive chromite from Brenham obviously yield high chromite/olivine ratios, but they also have relatively high troilite/olivine ratios (Wasson et al. 1999). At the other extreme, Phillips County, Hambleton, the chromite-free region of Brenham, Springwater, Krasnojarsk, and Thiel Mountains (all containing rounded olivine) as well as Glorieta Mountain, Newport, and Albin (common subgroup PMG) have high troilite/olivine ratios at low or zero chromite/olivine. Most PMG are near the origin, with Pavlodar (an anomalous member of the common subgroup that is also PMG-am) and Rawlinna (high-FeO PMG-as) having the lowest troilite/olivine (Fig. 4).

The two most sulfide-rich pallasites are noteworthy because of their anomalous olivine compositions which include fragmental olivine. The high-FeO PMG-as Phillips County has a highly heterogeneous metal composition (Wasson and Choi 2003). From its high troilite/metal ratio of ~5–10 (Scott 1977b), we conservatively estimate a value for the troilite/olivine ratio of ~0.5–1.0 (no olivine abundance is available in the literature). The low-MnO PMG Hambleton is similarly rich in sulfur (Johnson et al. 2006a, 2006b). Glorieta Mountain is an unusual pallasite in several respects: as well as a high sulfide content, it has heterogeneous olivine and chromite compositions (relative variation of more than 10% and 9%, respectively; Buseck and Goldstein 1969; Boesenberg et al. 2012); it has been classified as PMG-am for its low Ga, Ge, and Ir contents (Wasson and Choi 2003); it contains more radiogenic W (Quitté et al. 2005); and it had the lowest cooling rate at low temperatures of all pallasites investigated so far (Yang et al. 2010). Aside from high troilite contents, Albin and Newport are noteworthy only for their similarity to Glorieta Mountain in having heterogeneous chromite compositions (Wasson et al. 1999; Boesenberg et al. 2012; Fig. 3).

To Fig. 4, we have added contour lines indicating the distribution coefficient  $D_{\text{Mn}}$  which we define for the Mn sink and olivine (i.e., [sulfide or chromite]/olivine), in a simple partitioning model for a starting olivine composition with 0.3 wt% MnO (similar to common subgroup PMG) being modified to yield 0.2 wt% MnO (similar to low-MnO PMG). The identity of the phase

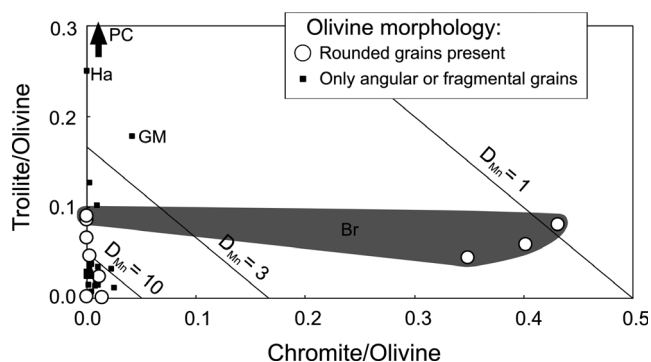


Fig. 4. Modal chromite/olivine and troilite/olivine for PMG from Buseck (1977) and Wasson et al. (1999; Brenham massive chromite). Contours for  $D_{Mn}$  (for [chromite or sulfide]/olivine) have been superimposed to illustrate required degree of chalcophile behavior to account for Mn concentrations in olivine from low-MnO PMG subgroup. Symbols and labeling of selected pallasites as for Figs. 2a and 3a.

that extracts Mn is not immediately important but does have petrological implications: in the case of sulfide, a melt can be removed after extracting Mn from olivine, while in the second, solid chromite is unlikely to be transported very far and would maintain the Mn locally in the newly formed low-MnO PMG region. In Fig. 4, one can see that only in the unlikely case of Mn being highly incompatible in olivine (i.e., highly chalcophile, with  $D_{Mn} \sim 10$ ) is it possible to explain the low-MnO PMG by Mn redistribution between olivine and the sink in approximately their observed abundances (and in any case, such high Mn levels are not observed in either troilite or chromite). If Mn were moderately incompatible in olivine ( $D_{Mn} \sim 1-3$ ), then there would be more capacity to produce the low-MnO PMG from the common subgroup PMG. However, Mn is unlikely to have been quite so chalcophile (Gaetani and Grove 1997; Li and Audétat 2012; Kiseeva and Wood 2013) and the high local abundance of massive chromite in certain parts of Brenham is not representative of the low-MnO PMG region. Large volumes of chromite probably had effective feeding zones across much larger scales of  $\sim 10-100$  cm (Wasson et al. 1999).

At more realistic Mn distribution values slightly less than unity (in our definition, moderately compatible in olivine and only slightly chalcophile; Kiseeva and Wood 2013), values for the sulfide/olivine or chromite/olivine ratios of  $\sim 0.5$  become reasonable for extracting sufficient Mn from the common subgroup PMG to produce the low-MnO PMG. Such a ratio probably only exists in the troilite-rich high-FeO PMG-as Phillips County (Scott 1977b). This implies that for realistic,

slightly chalcophile behavior for Mn, loss of a substantial amount of sulfide melt might conceivably explain the olivine composition in low-MnO PMG. Sulfide loss might have occurred either by a simple extraction at near-eutectic temperatures ( $\sim 950-1000$  °C; Raghavan 2004; Starykh and Sineva 2012) implying a bulk sulfide/olivine ratio of 0.5 for the precursor to the low-MnO PMG. Alternately, percolation of larger volumes of sulfide melt through the low-MnO PMG region could have occurred, and would be necessary if the  $D_{Mn}$  value was low (e.g., around  $\sim 0.1$ ). Percolation could occur by disseminated or channelized flow, the latter of which would act to increase the effective sulfide/olivine ratio locally. From their high troilite contents, Phillips County and Hambleton might be samples of trapped channelized sulfide melt. The very low sulfide abundance in most common subgroup PMG (Buseck 1977; Ulff-Møller et al. 1998) might be consistent with crystallization of metal around angular olivine in that region at high temperature, isolating these olivine grains and preventing rounding beyond the microscale (Scott 2017). Sulfide would then have been available for transport through the low-MnO PMG and high-FeO PMG-as regions to enable macroscale rounding in those areas. A high abundance of sulfide in the PMG parent body of around 10% is expected from the similarity of IIIAB and PMG metal geochemistry, and especially the partitioning behavior of highly siderophile elements that are sensitive to sulfur content in the melt (Chabot 2004; Goldstein et al. 2009; Boesenberg et al. 2012). The lack of troilite in most pallasites, but occasional troilite-rich specimens such as Phillips County, Hambleton, and Glorieta Mountain indicate concentration of sulfide into poorly sampled pockets. The low and very low cooling rates at low temperatures for Glorieta Mountain and Hambleton, respectively (Yang et al. 2010), further indicate that sulfide pockets or a small sulfide inner core might exist inside the PMG parent body (as suggested by Boesenberg et al. 2012). Such a core could be a significant sink for Mn in the PMG. These pallasites might be samples of a drainage channel feeding that core, or less likely could be samples of the core itself. Further evidence for large late structures in the PMG parent body might be indicated by a small compositional gap between chromites of the common subgroup PMG with the highest alumina contents and those of intermediate content, that is, between Ahumada and Otinapa, with the chromites of Glorieta Mountain lying on either side of this gap (Bunch and Keil 1971; Boesenberg et al. 2012;  $\sim Cr\# 87$  in Fig. 3). Interesting zoning in chromite from Otinapa and Newport (fig. 5 in Boesenberg et al. 2012) combined with their partially fragmental textures (Buseck 1977;

Scott 1977b; Haag 2003) might indicate potential for chromites to record transport of grains or liquids in breccia channels, or other more complex histories.

### Constraints on Planetesimal-Scale Differentiation and Melting Style

#### *Trace Element Geochemistry of Olivine and Metal*

An important question of interest for the PMG parent body, and for the parent bodies of nonchondrite meteorites in general, is whether they typically underwent bulk or fractional style melting (e.g., Boesenberg et al. 2012) and following from this, whether magma oceans of any significant depth formed at their surfaces (e.g., Wilson and Keil 2017). Here, we bring together some aspects of the available trace element data to present a synthesis of pallasite petrogenesis for the PMG parent body.

The simplest co-magmatic relationship between olivine in common subgroup PMG and that of high-FeO PMG-as would be a process of igneous fractionation, by either equilibrium or fractional crystallization (or alternately, melting to leave refractory olivine). However, on the basis of trace element analyses of olivine on various scales, it has been concluded that noisy trends defined by olivine from the common subgroup PMG do not extrapolate to that of the PMG-as (from whole- or intra-grain data using instrumental neutron activation analysis and EMPA; Mittlefehldt 1999, 2005; Mittlefehldt and Rumble 2006; Mittlefehldt and Herrin 2010; Boesenberg et al. 2012). The degree of fractionation is also unreasonably high for pallasites to represent a cumulate pile at the core-mantle boundary (e.g., ~33% from Sc; Mittlefehldt 1999). A simpler relationship was inferred from the mineralogy and mineral chemistry of low-MnO PMG and high-FeO PMG-as, in which some characteristics appear to be related by simple in situ reactions (Wasson and Choi 2003; Yang et al. 2010; Scott 2017).

Here, we would review two points on the relationship between the PMG subgroups from the perspective of lithophile element geochemistry. First, the difference between common (as well as low-MnO) PMG and high-FeO PMG is dictated in a general fashion by oxygen fugacity (Righter et al. 1990), with more magnesian olivine and metal richer in Fe existing at lower oxygen fugacities than more fayalitic olivine and metal poorer in Fe. Olivine and its coexisting metal may therefore have exchanged Fe at an early stage of planetesimal differentiation, simply as a function of available oxygen. In this model, the mantle or pallasite forming region was not fully depleted by melt extraction, because pyroxene or silicate melt must have been present in order to accommodate the additional

FeO and prevent wüstite production. This pyroxene or silicate melt has subsequently been lost from the PMG region, in a similar fashion to sulfide. In the PMG, those pyroxenes that are present appear to be secondary products crystallized as intergrowths with other accessory phases, and with only very low CaO contents (e.g., Buseck 1977; Boesenberg et al. 2012). This fine-grained pyroxene does not record the final widely distributed (and potentially Ca- and Al-bearing) parental silicate melt, but rather subsequent subsolidus reactions (Boesenberg et al. 2012) or very low degree remelting and sulfidation events. The signature of any parental silicate melt has therefore been obscured by interaction of olivine with metal-sulfide melt.

Second, although redox balance might qualitatively explain the high-FeO PMG-as and common (or low-MnO) PMG as silicate-metal reaction products with equivalent bulk compositions, the high abundance of farringtonite in the former complicates the model through addition of a phosphate component (Wasson and Choi 2003; Yang et al. 2010; Scott 2017). Oxidation of phosphorus from metal and repartitioning into a silicate melt is favored at lower temperature; this was previously suggested to have occurred in the solid state (Olsen and Fredriksson 1966) but is probably best enabled by trace oxygen in the metallic melt (Davis 1982; Kracher 1983). In the FeO-rich precursor to the PMG-as, reaction at lower temperature should strongly promote oxidation of phosphorus according to Equation 1 (Olsen and Fredriksson 1966; Fuchs 1967) enabling production of farringtonite and potentially phosphoran olivine. The presence of redox-related phosphate and phosphoran olivine in the absence of significant pyroxene strongly suggests, contrary to the assertion of Kracher (1983), that liquid metal can be the source of both phosphorus and oxygen. Both of these phases are also present in low-MnO pallasites but are rather rare by comparison to high-FeO PMG-as, and they are not known from the common PMG (Table 3; Fig. 2 and Table S4 in Data S1). Nevertheless, the textural, geochemical, and mineralogical correlations identified here indicate that the high-FeO PMG-as and the low-MnO subgroups may be more closely related than previously suspected. Full coverage of major and minor element geochemistry of olivine and chromite, and ultimately systematic lithophile trace element investigations of olivine and phosphate phases in all subgroups, will be required for more concrete interpretations.

A different perspective is available from the trace element geochemistry of metal. Although Ni contents of PMG metal are correlated with FeO content of olivine, replicate analyses of the same pallasites indicate that they are affected by sampling bias related to coarsely

crystalline kamacite-taenite exsolution (e.g., Scott 1977a; Wasson and Choi 2003). Some siderophile trace element analyses are also affected due to partitioning between these phases, and additionally into small accessory phases (e.g., Cu as native metal or in Cu-sulfide, and Cr in chromite: Buseck 1977; Wasson et al. 1999). Those siderophile elements that are less fractionated during subsolidus kamacite-taenite exsolution, especially Au and Ir, have been used to evaluate how primitive or evolved the metal might be in a simple model of fractional crystallization with occasional trapping of refractory solid metal (Wasson and Choi 2003). Other siderophile elements bring additional information to this scheme; the “anomalous metal” designation for some pallasites (PMG-am) combines several trace element peculiarities (e.g., Au-Ir systematics or Ga and Ge concentrations). Some are due to nonrepresentative sampling of the metal, while others might represent genuinely anomalous compositions. The PMG-am includes Argonia, Brenham, Glorieta Mountain, Huckitta, Krasnojarsk, Pavlodar (Wasson and Choi 2003), and Seymchan (Van Niekerk et al. 2007). In the following discussion, we will re-evaluate the classification and petrogenesis of the PMG-am.

Following Wasson et al. (1999) in using Au rather than Ni as an indicator of the degree of metal evolution, Wasson and Choi (2003) found that Krasnojarsk and Omolon have higher Co, As, and Sb with lower Ni and Cu than expected, suggestive of simply oversampling kamacite and undersampling taenite. Several of the PMG-am might be explained by sampling bias. In Fig. 5a, we plot Au versus Ir for bulk metal from PMG (most data from Wasson and Choi [2003] with some additional data from Scott 1977a; Lauretta et al. 2006; Sadilenko et al. 2006; Van Niekerk et al. 2007; Kissin et al. 2013). In the same figure, we also plot in situ analyses of discrete phases as crosses (indicating analytical errors) from PMG and the closely related IIIAB iron meteorite group (data from Mullane et al. 2004; Danielson et al. 2009). It can be seen that the phase with the highest concentration of Au in such meteorites is not kamacite or taenite, but probably a tiny accessory phase found so far in fine “plessite” mixtures or inclusions (labeled as taenite with inclusions by Danielson et al. 2009). This provides a possible new explanation for highly anomalous metal compositions found for Argonia and one replicate of Phillips County (Wasson and Choi 2003) as a mixture of mostly refractory Ir-rich and Au-poor metal with Ir-poor and Au-rich “plessite” (top-right of Fig. 5a). We suggest that the possible mixing field should be expanded to encompass the entire PMG data set. This would make production of the PMG and related anomalous IIIAB irons (Treysa quintet) from components similar to those

in IIIAB meteorites easier than previously suspected (Wasson and Choi 2003; Wasson 2016). If the in situ analyses of CMS 04071 by Danielson et al. (2009) are representative of PMG, then almost all pallasites seem to contain at least some of this plessite component, with the exception of analyses presented for Southampton, which seem to be practically separates of kamacite and taenite (Kissin et al. 2013; leftmost bulk metal analyses of Fig. 5a). Finally, it seems that the inclusion of a large amount of heterogeneously distributed, Au-rich and Ir-poor plessite or other highly evolved xenocrystic metal in Phillips County may also be consistent with its diverse texture including rounded, angular, and fragmental olivine, suggestive of a breccia channel that filled with troilite. Despite its high troilite content, the rounding of olivine might have been prevented simply by a high cooling rate through intermediate, near-solidus temperatures.

Other potentially important PMG-am examples are identified by anomalous concentrations of the volatile siderophile elements Ga and Ge. For their Au contents, Huckitta and Brenham have higher concentrations, while in Glorieta Mountain, they are lower; Wasson and Choi (2003) interpreted this to indicate volatility of Ga and Ge at high redox states, potentially induced locally by void space within the parent body. On an in situ basis, only CMS 04071 has been investigated for these elements, with chromite found to be the main host for Ga (Danielson et al. 2009). As for most trace lithophile elements in olivine, more complete coverage will be helpful in understanding the geochemistry of Ga and Ge of pallasites and the potential for tracing gas pressures and void space in the PMG parent body.

The conspicuous PMG-am Pavlodar is unlike the other common subgroup PMG in several characteristics. Pavlodar contains olivine with a Fa-content typical for the common PMG subgroup (Buseck 1977; Scott 1977b;  $\sim\text{Fa}_{12.5-12.7}$  with the normal range being  $\text{Fa}_{11-14}$ ), but this olivine is of the rounded variety and has a higher MnO content (0.35–0.37 wt%, as opposed to 0.32 wt% or lower in most other PMG with similar Fa-contents; Smith et al. 1983; Boesenberg et al. 2012). Pavlodar olivine cores contain Cr-rich exsolution features and therefore high bulk olivine Cr contents ( $\sim 550\text{--}600$  ppm from Steele 1994; Mittlefehldt 1999) indicative of a potentially homogeneous Cr content at high temperature that later exsolved at lower temperature. This olivine is hosted in metal with a primitive, Ni- and Au-poor, Ir- and Pt-rich composition with chondritic Ga/Ge, indicating a potential parental metallic liquid (Scott 1977a; Wasson and Choi 2003). Chromite in this pallasite is nearly Al-free (Boesenberg et al. 2012), similar to the low- $\text{Al}_2\text{O}_3$  chromites in low-MnO PMG

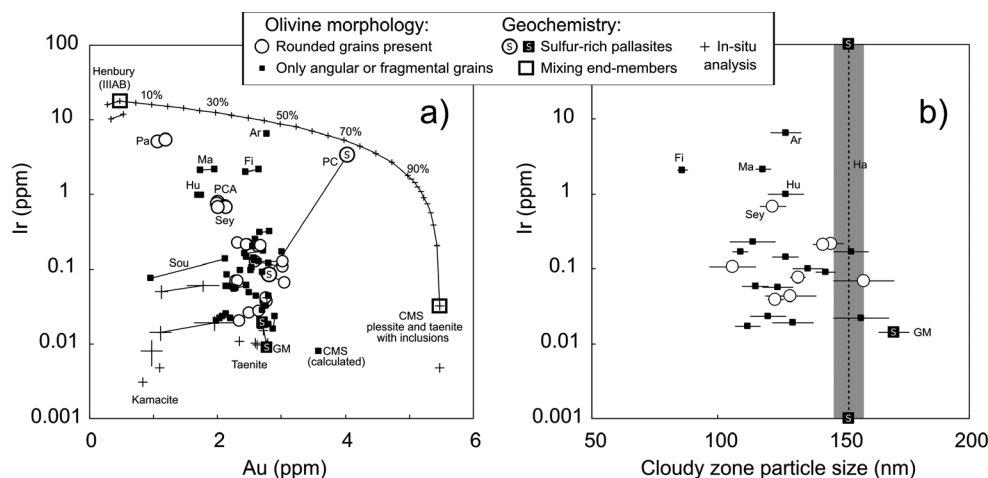


Fig. 5. a) Au and Ir bulk metal PMG concentrations (Wasson and Choi [2003] with some additional data from Scott 1977a; Lauretta et al. 2006; Sadilenko et al. 2006; Van Niekerk et al. 2007; and Kissin et al. 2013) and in situ analyses of kamacite, taenite, and plessite for PMG (Brenham) and closely related IIIAB irons (Mullane et al. 2004; Danielson et al. 2009). In situ analyses of these materials are indicated by crosses with the lengths of each arm indicating analytical error (in Mullane et al. 2004; Danielson et al. 2009) and labeled in the figure. Following Wasson and Choi (2003), we have added a mixing line between primitive and evolved endmembers, but use more recent measurements from Henbury IIIAB taenite and CMS 04071 plessite as endmembers. The mixing curve is labeled with the percentage of the plessite and taenite component. Sulfide-rich pallasites are indicated by “S” inside the symbol. All other symbols are as for Figs. 2a and 3a, and replicates of the same pallasite are indicated by tie-lines. b) Cloudy zone particle size (Yang et al. 2010) versus bulk Ir analyses (Wasson and Choi 2003; Van Niekerk et al. 2007) for PMG samples. Symbols as for (a). Selected pallasites are labeled following Figs. 2–4, with the following additional abbreviations: Argonia (Ar); Huckitta (Hu); Finmarken (Fi); Pecora Escarpment 91004 (PCA).

(of which it is not a member) and also near to pure chromite in IIIAB iron meteorites (Olsen et al. 1999). This indicates that it crystallized almost entirely from liquid metal (Ulff-Møller 1998b; Wasson et al. 1999). Despite these unusual characteristics, the oxygen isotope compositions of Pavlodar are within the normal range for PMG, strongly suggesting origin in the same planetesimal source (Greenwood et al. 2015).

The presence of rounded olivine in Pavlodar is a potentially important environmental indicator. Solferino et al. (2015) summarized the controls on wetting of olivine by metal-sulfide melts, indicating that S-, Ni-, and O-poor melt is the least likely to be interconnected by high dihedral angles. Rounding and grain growth in the case of Pavlodar is therefore unexpected, or may represent the most primitive metallic melt composition capable of generating relatively large rounded olivines (scale of several millimeters; Scott [1977b] and references therein; Steele 1994), with more primitive metallic melts becoming trapped as inclusions in olivine grains or in triple junctions in olivine aggregates. The duration of grain growth and rounding of ~0.1 Myr found by Solferino et al. (2015) may therefore be a lower limit for Pavlodar. Yang et al. (2010) identified Pavlodar as a potential “core–mantle” boundary sample in the classical case of quiescent and fully separated core and mantle domains. If the metal in Pavlodar represents the most primitive fully interconnected

metallic melt, then its anomalous olivine composition may be consistent with more efficient silicate melt extraction. Additionally, in situ equilibrium crystallization of primitive metallic melt might have prevented oxidation of phosphorus (via concentration of oxygen in fractionally crystallized metallic melt) and explains the lack of farringtonite and phosphoran olivine that are found in other pallasites with rounded olivine (Scott 2017). Those pallasites with metal compositions that are most similar to Pavlodar also lack farringtonite and phosphoran olivine, consistent with this process (e.g., Argonia, Finmarken, Huckitta, Marjalahti, Pecora Escarpment 91004, and Seymchan). Aside from the lack of phosphate-bearing phases in primitive metal, there is no obvious relationship among the PMG between Ir-Au metal systematics and the other correlations that we have identified in this study, namely olivine texture, olivine composition, and type of accessory phases (Al-free or Al-bearing chromite, the various phosphates, and phosphoran olivine).

Boesenberg et al. (2012) highlighted the potential importance of incomplete melting scenarios in modeling pallasite petrogenesis. In low-degree fractional melting of a planetesimal that fails to produce a deep magma ocean or complete metal-silicate separation, it is expected that primitive, refractory, high-Ir metal would be preserved in the middle or upper mantle (Scott 2017). Pallasites with higher Ir than expected for their

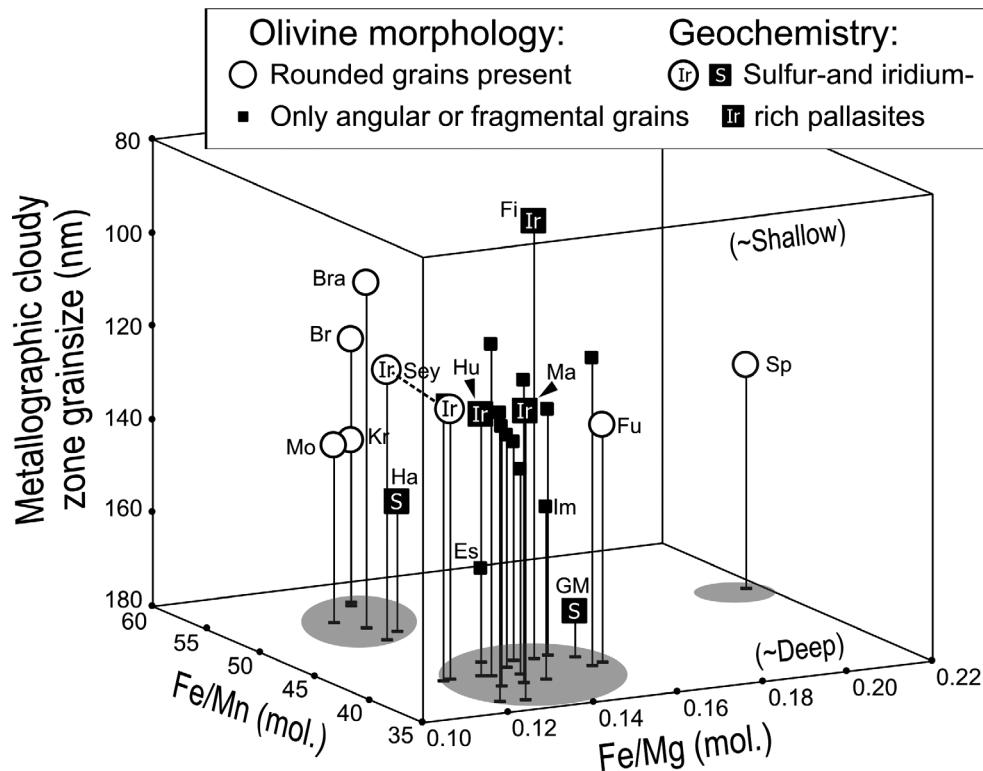


Fig. 6. Olivine molar Fe/Mg, Fe/Mn, and metallographic cloudy zone grain size (as a proxy for cooling rate) for available PMG plotted with symbols from Fig. 5. The scale for cloudy zone grain size has been inverted to reflect more rapid cooling resulting in finer exsolution grain size near the surface of a postulated parent body, and slower cooling resulting in coarser grain size in the interior. Replicates of Seymchan (which occur in both common and low-MnO subgroups) are connected with a dotted line. Sulfide- and iridium-rich pallasites are indicated by “S” and “Ir” inside symbols, respectively.

other metal trace element contents such as Argonia, Finmarken, Marjalahti, and one replicate of Phillips County record a mixture of exactly such refractory, solid metal with more evolved liquid metal compositions (Fig. 5a; Wasson and Choi 2003). The Ir-Au systematics do not require input of foreign metal; all analyses seem to be consistent with mixtures of early and late components. This was suggested to have occurred during catastrophic mixing (Wasson and Choi 2003) but could also have occurred by migration of metal partial melts from different parts of the planetesimal while solid Ir-rich metal grains remained stationary in an olivine framework. In addition, preliminary findings for triple-oxygen isotope systematics show no resolvable difference in mass-independent components between the IIIAB and PMG parent bodies, as recorded by chromites in the former and olivine in the latter (i.e., no obviously foreign material; Franchi et al. 2013). Instead, recent data from Ali et al. (2018) indicate that some relationship may exist between modal proportion of olivine and oxygen isotopes within the PMG. Although this is an area of active and ongoing investigation, at this stage these data suggest a scenario in which foreign

metal need not be introduced, but rather that high degrees of melting occurred in which complete melting of metal and silicate was never reached.

#### *Paleomagnetic, Cooling Rate, and Isotopic Constraints on the Evolution and Final Structure of the PMG Parent Body*

Several pallasites have been shown to record the former presence of a magnetosphere upon cooling through the Curie temperatures of tiny inclusions in olivine and of microstructures in metal (Tarduno et al. 2012; Bryson et al. 2015; Nichols et al. 2016). These paleofields were suggested to have been imparted by a dynamo present during one or more stages of core evolution, from a possible early thermally driven regime (a fully liquid, convecting core), a compositionally driven regime (a partially molten, crystallizing core), or a late remnant field preserved in the solid core or nearby rocky material. High and decreasing paleofield intensities were recorded in Imilac and Esquel by inclusions in olivine and in “cloudy zone” exsolved nanometer-scale tetrataenite inclusions hosted within ordered  $\text{Fe}_3\text{Ni}$  metal ( $\sim 120 \mu\text{T}$  in the former, and

~80  $\mu\text{T}$  decreasing to the detection limit of ~10  $\mu\text{T}$  in the latter; Bryson et al. 2015). By contrast, low or zero paleofield intensities were found for Brenham and Marjalahti from cloudy zone exsolved tetrataenite alone (~10  $\mu\text{T}$  or lower; Nichols et al. 2016). In these investigations, the thermal histories of these meteorites were interpreted in the context of a relatively simple structure comprising a fully segregated liquid core with overlying mantle, leading to a model in which a 200 km radius conductive planetesimal cooled over a period of ~250 Myr. Nichols et al. (2016) used metallographic cooling rates from Yang et al. (2010) to infer depths and a chronological order of cooling. Higher cooling rates for Brenham and Marjalahti, from cloudy zone particle sizes of  $123 \pm 3$  and  $118 \pm 3$  nm, respectively, correspond to  $6.2 \pm 0.9$  K/Myr in the former (2 SEs). These were taken to indicate that Brenham and Marjalahti were high in the mantle and reached closure relatively early. Lower cooling rates for Imilac and Esquel, from coarser cloudy zone particle sizes of  $143 \pm 4$  and  $157 \pm 11$  nm, respectively, indicated a position lower in the mantle (although not near the core–mantle boundary) and that they reached closure later. In this model, an early magnetosphere driven by thermal convection predated a period of dynamo quiescence, and Brenham and Marjalahti reach closure in the mid-upper mantle during this inactivity. Subsequently, a crystallization-driven regime took over, powering a strong magnetosphere in which Imilac and finally Esquel reach closure sometime in the next 100 Myr or more (Nichols et al. 2016). The need to thermally isolate the pallasitic region from the outward-crystallizing core led to the conclusion that pallasites formed in the upper or mid-mantle and that the metal was foreign, with locally high Ir concentrations taken as support (supplementary material for Tarduno et al. 2012).

In the PMG, there are local enhancements of Ir indicating that complete melting of metal never occurred (Boesenberg et al. 2012) and no clear triple-oxygen isotopic evidence yet for large mass-independent variation associated with potentially foreign chemistry or mineralogy (thus far only with olivine content; Ali et al. 2018) nor with chromites in closely related IIIAB metal (indistinguishable from olivine; Franchi et al. 2013; Greenwood et al. 2015). Although this is an area of active investigation, we tentatively suggest an alternative interpretation of the paleomagnetic data. At peak temperatures, the PMG metal was subliquidus and the parent body was already in the compositional (crystallization) driven convective regime. Following Boesenberg et al. (2012), the presence of refractory Ir-rich metal in the pallasitic mantle suggests that the pallasitic region was thick and overlying a partially

molten, inwardly crystallizing core. There is a slight tendency for high-Ir PMG to have only moderately coarse (Argonia, Marjalahti, Huckitta, and Semychan at ~125 nm) or fine (Finmarken  $86 \pm 2$  nm) cloudy zone microstructures, while sulfide-rich pallasites are among those pallasites with the coarsest cloudy zone microstructures and therefore the lowest cooling rates (Glorieta Mountain and Hambleton, at  $170 \pm 6$  and  $152 \pm 6$  nm, respectively). These data are illustrated in Fig. 5b, in which it can be seen that the relationship used by Boesenberg et al. (2012) to argue that metal crystallization in the pallasite region occurred from outside to inside, is in fact more subtle than originally implied because of considerable noisy scatter in cloudy zone grain size or geochemistry of the metal. Nevertheless, the aforementioned relationship appears robust and indicates that late sulfide was mobile and concentrated at greater depths in the PMG parent body (Boesenberg et al. 2012). However, the stepwise nature of cooling in the PMG parent body (e.g., Fowler-Gerace and Tait 2015) indicates that the cooling path of any particular package of pallasitic material at high temperature need not correspond perfectly to its cooling rates at low temperature. Features obtained during magmatic evolution (including crystallization of metallic melts, grain growth and rounding of olivine, and accessory phase mineralogy all being set at ~1000 °C or higher) formed at least several million years before those obtained during cooling at low temperatures (appropriate for generation of metallographic textures, recording of cooling rates and paleomagnetic fields, as well as fission track dating taking place at ~400–600 °C). Systematic fission track dating of pallasites seems especially promising for dating the cooling rates obtained from metallographic textures, although from only five pallasites a bimodal distribution of ages has been found (4.37 and ~4.2 Ga) that is so far uncorrelated with the size of cloudy zone microstructures (Pellas et al. 1983; Bondar and Perelygin 2003). The large difference in temperature and time between magmatic and metallographic cooling stages in the evolution of the PMG parent body, and the long interval required to approach those low cooling rates, implies a more complex planetesimal history in the intervening period.

Rather than invoking the input of foreign metal into the surface of the PMG parent body, we suggest removing this requirement and instead propose a degree of local geological complexity to explain the scattered tendencies in Fig. 5b. There are possible planetesimal scale features that might explain the presence of cold pallasitic material capable of recording a magnetic field, lying in proximity to its native, partially molten convecting core. This arrangement must achieve thermal isolation of the pallasitic region from the partially liquid

core, that is, a steeper geothermal gradient in the metal-silicate mixture, or use local amplification of a very weak magnetic field in the core. Both might occur through the presence of large structures in a highly evolved, complex planetesimal. The simplest cases of thermal isolation involve a thick, continuous silicate mantle to provide insulation (Tarduno et al. 2012; Bryson et al. 2015; Nichols et al. 2016) or residence in a porous megaregolith, although a near-surface impact-generated regolith seems unlikely considering the limited evidence for late shock processing. Any early substructure in olivine crystal lattices may have been erased by subsequent recovery, especially in those pallasites containing rounded olivine (Matsui et al. 1980; Mori 1986; Desrousseaux et al. 1997). Springwater exhibits an early preferential alignment of olivine (Fowler-Gerace et al. 2016) and if this is confirmed in other similar pallasites, it would have important tectonic implications. In order to increase the thermal gradient, more useful types of porosity might include cavities in which Ga and Ge could have become volatile (Wasson and Choi 2003) and emptied breccia channels that might have enabled drainage of sulfide into the interior as the planetesimal adjusted to lower temperature (indicated by low cooling rates for sulfide-rich pallasites; Fig. 5b). Such void space was suggested to be possible via contraction of the metal relative to olivine during cooling (Wasson and Choi 2003). The observation of preferential kink banding deformation in angular olivine rather than rounded suggests that those pallasites containing rounded olivine somehow accommodated small degrees of deformation, perhaps by expulsion of very low degree interconnected melts (Klosterman and Buseck 1973; Fowler-Gerace et al. 2016). These kink bands probably formed at low to intermediate temperatures, perhaps close to or slightly higher than that of kamacite-taenite exsolution (Klosterman and Buseck 1973).

A further scenario that might help reconcile the various pallasite characteristics has been opened by the possibility of immiscibility between sulfide- and phosphide-rich melts, suggested by regions in Brahin in which only a single accessory mineral occurs (Figs. 1a and 1b). Separation of Fe-Ni-phosphide melt by immiscibility may enable partial melts to persist to lower temperatures, until finally reaching the Ni-phosphide eutectic in the range 850–875 °C (Doan and Goldstein 1970) or even lower if additional soluble elements are present in the concentrated melt. The weak magnetic field associated with such a tiny inward-crystallizing metal-phosphide core could be locally modified by massive channels of metal (e.g., olivine-free regions in Brenham, Glorieta Mountain, and Szymchan) or sulfide (Glorieta Mountain, Hambleton, and Phillips County) with possible amplification by a factor of 3–200 in proximity to extreme

morphologies (Bryson et al. 2015). Core crystallization occurring from the outside toward the inside may therefore generate a weak magnetic field that could be locally enhanced by structures in the planetesimal to be recorded by pallasitic material in appropriate locations, for example, Esquel and Imilac residing in solid metal, perhaps in a dendrite. The additional question of whether the IIIAB irons are closely or more distally related to PMG metal has also been recently addressed by cooling rate information. Although the Ni-rich end of the IIIAB sequence is geochemically very similar to the PMG metal, the latter seems to have crystallized in its parent body from the outside to the inside (Boesenberg et al. 2012; Fig. 5b) and the cooling rates the IIIAB irons are higher than those of the PMG (Yang and Goldstein 2006; Yang et al. 2010). This is inconsistent with a simple planetesimal comprising PMG material overlying a IIIAB core. Therefore, we only suggest that components in IIIAB irons are similar or analogous to those in PMG metal. They may nevertheless be related through formation in an even earlier precursor planetesimal, or represent a mixture of two planetesimals (e.g., Yang et al. 2010), or ultimately have inherited a common trace element inventory from the same part of the solar nebula.

The above short history involving rapid early cooling from high to moderate temperatures is supported by short- and long-lived radiogenic isotope studies that indicate rapid pallasite formation and cooling to subsolidus temperatures (e.g., Al-Mg, Mn-Cr, Hf-W, Ag-Pd, and Re-Os). The isotope systematics of lithophile elements in pallasites diverged from chondritic behavior very early. From the Al-Mg decay system, silicate differentiation and isolation of PMG olivine from aluminous melt occurred at 1.24 (+0.40/–0.28) Myr after solar system formation (Baker et al. 2012). Similarly, rapid cooling of the PMG parent body is indicated by Mn-Cr isotope systematics, yielding diffusive closure of Mn and Cr in olivine of Omolon and Springwater within ~10 Myr of solar system formation (Lugmair and Shukolyukov 1998), and possible cooling to near-solidus conditions and segregation of low-degree Mn-rich melts in Brahin and Brenham within ~2.5 to 4 Myr (McKibbin et al. 2016). For the lithophile-siderophile Hf-W decay scheme, W-deficit dating methods have undergone considerable revision due to correction for exposure in space (e.g., Kruijer et al. 2014). Despite this, the available data for the PMG parent body metal-silicate differentiation event seem to have been at a similarly early period to most other iron meteorites, except for the more radiogenic Glorieta Mountain (Quitté et al. 2005). This may be consistent with the slow cooling rate of this pallasite at low temperature (Yang et al. 2010) and its angular olivine and variable mineral geochemistry (Boesenberg

et al. 2012). A very similar timescale is indicated for the PMG by the purely siderophile Pd-Ag system, which indicates metal fractionation and isolation of most PMG within ~12 Myr of solar system formation. Lower precision chronological information for Re-Os give ages of  $60 \pm 40$  Myr (Shen et al. 1998; Chen et al. 2002). The Re-Os ages might indicate slow closure or later disturbance for this particular system at relatively low temperature. Taken together, the radiogenic isotope ages are more consistent with rapid cooling, rather than the long timescales of simple cooling models used to interpret paleomagnetic data (~100 Myr or longer: Tarduno et al. 2012; Bryson et al. 2015; Nichols et al. 2016). They are therefore encouraging for a planetesimal model involving refractory metal trapped throughout the mantle and a small crystallizing liquid inner core.

### CONCLUSIONS

Among the PMG, there is a strong correlation between olivine morphology, specifically the existence of “macroscale” rounded olivine (diameter ~5–15 mm; Scott 1977b), and anomalous characteristics (e.g., PMG-am and high-FeO PMG-as; Kissin 2008, 2009) including low MnO contents of olivine (e.g., Boesenberg et al. 2012; McKibbin et al. 2016). In the high-FeO PMG-as and the low-MnO PMG subgroups, the MgO-rich and phosphorus-bearing phases farringtonite and phosphoran olivine occur with low- $\text{Al}_2\text{O}_3$  chromite and rounded olivine. Large (diameter ~5 mm or more) rounded olivine morphologies and the presence of farringtonite and phosphoran olivine indicate prolonged interaction between silicate and metallic reservoirs in the PMG parent planetesimal, with phosphorous, chromium, and oxygen sourced from the metallic liquid. These minerals might therefore be indicators of genuine core–mantle boundaries or core–mantle interaction zones. The prior removal of silicate melt at the planetesimal’s peak temperature (between eutectic melting at 1050–1100 °C and upper limits of 1600–1700 °C; Boesenberg et al. 2012) indicates that farringtonite and low- $\text{Al}_2\text{O}_3$  chromite formed by back-reaction during retrograde cooling (to ~1000 °C; e.g., Brunet and Laporte 1998). This occurred via oxidation of phosphorus and chromium, which are siderophile at high temperatures but lithophile at lower, near-solidus temperatures.

Farringtonite and phosphoran olivine are not present in the more populous common subgroup PMG (i.e., most pallasites), which may be simple mechanical mixtures of olivine, Al-bearing chromite, primitive metal xenocrysts, and more evolved liquid metal. Large olivine masses or disaggregated olivine crystals hosted in metal may be typical of the “middle mantle” of the pallasite parent body intruded by variably evolved metal (Boesenberg

et al. 2012) over various depths (Yang et al. 2010). However, because magmatic temperatures are far above kamacite-taenite exsolution temperatures, this may mask a long interval in pallasite history, and significant geological noise has been superimposed upon the relationships described above through an erratic, stepwise cooling history (Fowler-Gerace and Tait 2015). The Pavlodar pallasite seems to be an early isolate of highly refractory metal, perhaps separated at an early stage, at peak melting and melt extraction.

The geochemistry of Mn in olivine and chromite, particularly the low concentrations in olivine of the low-MnO PMG and high concentrations in low- $\text{Al}_2\text{O}_3$  chromites, traces the former presence of sulfide melt in pallasites and partially chalcophile nature of Mn. Due to fractional crystallization of the metallic liquid, it is likely that a small liquid sulfide inner core, and possibly a very small liquid phosphide inner core, developed in the PMG parent body due to fractional crystallization and liquid immiscibility. Such a small inner core might generate a weak and locally variable dynamo responsible for paleomagnetic signatures in some pallasites (e.g., Tarduno et al. 2012).

The geochemical behavior of Mn in pallasitic environments may be similar across multiple planetesimals. The PES group, although originating in a different parent body in a very different part of the solar system (Clayton and Mayeda 1978, 1996; Warren 2011), shares a very similar accessory phase mineralogy, including Mn-bearing phosphate minerals and troilite. In the PES Yamato 8451, olivine rims are enriched in Mn and have a lower fayalite content than their cores, suggestive of repartitioning or new crystallization during cooling (Miyamoto 1997). For the low-MnO PMG pallasites, a Mn-rich silico-phosphate liquid was suggested to control the late Cr-isotope evolution of such parent bodies, with  $^{53}\text{Mn}$ – $^{53}\text{Cr}$  decay generating isotopic anomalies in interstitial phases and olivine rims (McKibbin et al. 2016). The partially chalcophile behavior of Mn may provide another mechanism by which the fractionation of Mn on planetary scales could occur, with sequestration of Mn along with sulfide in pockets in the interior or in the inner cores of planetesimals (suggested by sulfide-rich pallasites with low cooling rates, such as Glorieta Mountain and Hambleton; Yang et al. 2010).

*Acknowledgments*—We thank the Royal Belgian Institute of Natural Sciences (RBINS) for loan of samples Brahin, Esquel, and Imilac; the Meteorite Working Group (NASA-MWG) for loan of CMS 04071; the Research School of Earth Sciences, Australian National University for loan of a sample of Brenham; Luc Deriemaeker (VUB Belgium) and Peter Czaja (NKM Berlin Germany) for help with analysis

and data processing; and Maxwell Brown for useful discussions about paleomagnetism. We also thank Richard Windmill, Joseph Boesenberg, Ed Scott, Neva Fowler-Gerace, and one anonymous reviewer for their critical reviews and suggested improvements to the manuscript. This research was supported by Planet TOPERS, an initiative of the Belgian Science Policy Office (BELSPO), and by a fellowship from the Research Foundation—Flanders (Fonds Wetenschappelijk Onderzoek—Vlaanderen; FWO—project 1209515N) to S. McK., who is currently a postdoctoral fellow of the Alexander von Humboldt Foundation.

*Editorial Handling*—Dr. Edward Scott

## REFERENCES

- Agee C. B., Ziegler K., and Muttik N. 2015. New unique pyroxene pallasite: Northwest Africa 10019. *Meteoritical Society Meeting* 78:5084.
- Ali A., Jabeen I., Banerjee N. R., Osinski G. R., Nicklin I., Gregory D., and Herrmann P. 2018. The oxygen isotope compositions of olivine in main group (MG) pallasites: New measurements by adopting an improved laser fluorination approach. *Meteoritics & Planetary Science* 53:1223–1237.
- Ando J. 1958. Phase diagrams of  $\text{Ca}_3(\text{PO}_4)_2$ – $\text{Mg}_3(\text{PO}_4)_2$  and  $\text{Ca}_3(\text{PO}_4)_2$ – $\text{CaNaPO}_4$  systems. *Bulletin of the Chemical Society of Japan* 31:201–205.
- Atkinson H. V. 1988. Theories of normal grain growth in pure single phase systems. *Acta Metallurgica* 36:469–491.
- Baker J. A., Schiller M., and Bizzarro M. 2012.  $^{26}\text{Al}$ – $^{26}\text{Mg}$  deficit dating ultramafic meteorites and silicate planetesimal differentiation in the early solar system? *Geochimica et Cosmochimica Acta* 77:415–431.
- Bell J. F., Davis D. R., Hartmann W. K., and Gaffey M. J. 1989. Asteroids: The big picture. In *Asteroids II*, edited by Binzel R. P., Gehrels T., and Matthews M. S. Tucson, Arizona: University of Arizona Press. pp. 921–945.
- Boesenberg J. S. and Hewins R. H. 2010. An experimental investigation into the metastable formation of phosphoran olivine and pyroxene. *Geochimica et Cosmochimica Acta* 74:1923–1941.
- Boesenberg J. S., Davis A. M., Prinz M., Weisberg M. K., Clayton R. N., and Mayeda T. K. 2000. The pyroxene pallasites, Vermillion and Yamato 8451: Not quite a couple. *Meteoritics & Planetary Science* 35:757–769.
- Boesenberg J. S., Delaney J. S., and Hewins R. H. 2012. A petrological and chemical re-examination of main group pallasite formation. *Geochimica et Cosmochimica Acta* 89:134–158.
- Boesenberg J. S., Humayun M., Windmill R., Greenwood R. C., and Franchi I. A. 2018. Sericho: A new main group Pallasite with two types of chromite (abstract #1556). 49th Lunar and Planetary Science Conference. CD-ROM.
- Bondar Y. V. and Pereygin V. P. 2003. Cosmic history of some pallasites based on fossil track studies. *Radiation Measurements* 36:367–373.
- Brunet F. and Laporte D. 1998. Phosphorus behaviour in pallasites: Experimental constraints. *Goldschmidt Conference Toulouse, Mineralogical Magazine* 62A:252–253.
- Bryson J. F. J., Nichols C. I. O., Herrero-Albillos J., Kronast F., Kasama T., Alimadadi H., van der Laan G., Nimmo F., and Harrison R. J. 2015. Long-lived magnetism from solidification-driven convection on the pallasite parent body. *Nature* 517:472–475.
- Bunch T. E. and Keil K. 1971. Chromite and ilmenite in non-chondritic meteorites. *American Mineralogist* 56:146–157.
- Bunch T. E., Rumble D. III, Wittke J. H., and Irving A. J. 2005. Pyroxene-rich pallasites Zinder and NWA 1911: Not like the others (abstract #5219). *Meteoritics & Planetary Science* 40.
- Buseck P. R. 1977. Pallasite meteorites—Mineralogy, petrology and geochemistry. *Geochimica et Cosmochimica Acta* 41:711–740.
- Buseck P. R. and Clark J. 1984. Zaisho—A pallasite containing pyroxene and phosphoran olivine. *Mineralogical Magazine* 48:229–235.
- Buseck P. R. and Goldstein J. I. 1969. Olivine compositions and cooling rates of pallasitic meteorites. *Geological Society of America Bulletin* 80:2141–2158.
- Buseck P. R. and Holdsworth E. 1977. Phosphate minerals in pallasite meteorites. *Mineralogical Magazine* 41:91–102.
- Chabot N. L. 2004. Sulfur contents of the parental metallic cores of magmatic iron meteorites. *Geochimica et Cosmochimica Acta* 68:3607–3618.
- Chabot N. L. and Drake M. J. 2000. Crystallization of magmatic iron meteorites: The effects of phosphorus and liquid immiscibility. *Meteoritics & Planetary Science* 35:807–816.
- Chen J. H., Papanastassiou D. A. and Wasserburg G. J. 2002. Re-Os and Pd-Ag systematics in Group IIIAB irons and in pallasites. *Geochimica et Cosmochimica Acta* 66:3793–3810.
- Chernozhukhin S. M., Weyrauch M., Goderis S., Oeser M., McKibbin S. J., Horn I., Hecht L., Weyer S., Claeys P., and Vanhaecke F. 2017. Thermal equilibration of iron meteorite and pallasite parent bodies recorded at the mineral scale by Fe and Ni isotope systematics. *Geochimica et Cosmochimica Acta* 217:95–111.
- Clark R. S. Jr. and Goldstein J. I. 1978. Schreibersite growth and its influence on the metallography of coarse-structures iron meteorites. *Smithsonian Contribution to the Earth Sciences* 21:1–77.
- Clayton R. N. and Mayeda T. K. 1978. Genetic relations between iron and stony meteorites. *Earth and Planetary Science Letters* 40:168–174.
- Clayton R. N. and Mayeda T. K. 1996. Oxygen isotope studies of achondrites. *Geochimica et Cosmochimica Acta* 60:1999–2017.
- Coogan L. A., Saunders A. D., and Wilson R. N. 2014. Aluminum-in-olivine thermometry of primitive basalts: Evidence of an anomalously hot mantle source for large igneous provinces. *Chemical Geology* 368:1–10.
- Cooper T. D. 1974. Elemental abundances in the silicate phase of pallasitic meteorites. Unpublished M.S. thesis, Oregon State University.
- Coutinho J. M. V., Quitete E. B., and de Oliveira M. C. B. 1999. The Quijingue meteorite: A pallasite from Bahia, Brazil. *Revista Brasileira de Geociências* 29:447–448.
- Danielson L. R., Richter K., and Humayun M. 2009. Trace element chemistry of Cumulus Ridge 04071 pallasite with implications for main group pallasites. *Meteoritics & Planetary Science* 44:1019–1032.

- Davis A. M. 1982. Phosphorus in main group pallasites. *Meteoritics* 17:203.
- Davis A. M. and Olsen E. J. 1991. Phosphates in pallasite meteorites as probes of mantle processes in small planetary bodies. *Nature* 353:637–640.
- Davis A. M. and Olsen E. J. 1996. REE patterns in pallasite phosphates—A window on mantle differentiation in parent bodies. *Meteoritical Society Meeting* 31:A34–A35.
- DellaGiustina D. N., Lauretta D. S., Hill D. H., Killgore M., Yang H., and Downs R. T. 2011. Implications of the presence of tridymite in the Fukang pallasite (abstract #1915). 42nd Lunar and Planetary Science Conference. CD-ROM.
- DellaGiustina D. N., Habib N., Domanik K. J., Hill D. H., Lauretta D. S., Goreva Y. S., Killgore M., Hexiong Y., and Downs R. T. 2019. The Fukang pallasite: Characterization and implications for the history of the Main-group parent body. *Meteoritics & Planetary Science* 54:1781–1807.
- Desrousseaux A., Doukhan J. C., Leroux H., and Van Duysen J. C. 1997. An analytical electron microscope investigation of some pallasites. *Physics of the Earth and Planetary Interiors* 103:101–115.
- Doan A. S. and Goldstein J. I. 1970. The ternary phase diagram, Fe-Ni-P. *Metallurgical Transactions* 1:1759–1767.
- Donohue P. H., Hill E., and Huss G. R. 2018. Experimentally determined subsolidus metal-olivine element partitioning with applications to pallasites. *Geochimica et Cosmochimica Acta* 222:305–318.
- Drake M. J., Newsom H. E., and Capobianco C. J. 1989. V, Cr, and Mn in the Earth, Moon, EPB, and SPB and the origin of the Moon: Experimental studies. *Geochimica et Cosmochimica Acta* 53:2101–2111.
- Dufresne E. R. and Roy S. K. 1961. A new phosphate mineral from the Springwater pallasite. *Geochimica et Cosmochimica Acta* 24:198–205.
- Fowler-Gerace N. A. and Tait K. T. 2015. Phosphoran olivine overgrowths: Implications for multiple impacts to the Main Group pallasite parent body. *American Mineralogist* 100:2043–2052.
- Fowler-Gerace N. A., Tait K. T., Moser D. E., Hyde B. C., and Barker I. 2013. Mineralogical investigation of the phosphorus-rich Springwater pallasite. *Meteoritical Society Meeting* 76:5276.
- Fowler-Gerace N. A., Tait K. T., Moser D. E., Barker I., and Tian B. Y. 2016. Aligned olivine in the Springwater pallasite. *Meteoritics & Planetary Science* 51:1125–1135.
- Franchi I. A., Greenwood R. C., and Scott E. R. D. 2013. The IIIAB-Pallasite relationship revisited: The oxygen isotope perspective. *Meteoritical Society Meeting* 76:5326.
- Francis C. A. and Lange D. E. 1987. A new olivine-chromite assemblage in the Brenham pallasite. *Geological Society Abstracts Programme* 19:667.
- Fuchs L. H. 1967. Stanfieldite: A new phosphate mineral from stony-iron meteorites. *Science* 158:910–911.
- Fuchs L. H. 1969. The phosphate mineralogy of meteorites. In *Meteorite research*, edited by Millman P. M. Dordrecht, the Netherlands: Reidel. pp. 683–95.
- Fuchs L. H., Olsen E., and Gebert E. 1973. New X-ray and compositional data for farringtonite,  $Mg_3(PO_4)_2$ . *American Mineralogist* 58:949–951.
- Gaetani G. A. and Grove T. L. 1997. Partitioning of moderately siderophile elements among olivine, silicate melt, and sulfide melt: Constraints on core formation in the Earth and Mars. *Geochimica et Cosmochimica Acta* 61:1829–1846.
- Gaetani G. A. and Grove T. L. 1999. Wetting of mantle olivine by sulfide melt: Implications for Re/Os ratios in mantle peridotite and late-stage core formation. *Earth and Planetary Science Letters* 169:147–163.
- Goldstein J. I., Scott E. R. D., and Chabot N. L. 2009. Iron meteorites: Crystallization, thermal history, parent bodies, and origin. *Chemie der Erde* 69:293–325.
- Goodrich C. A. 2003. Petrogenesis of olivine-phyric shergottites Sayh al Uhaymir 005 and Elephant Moraine A79001 lithology A. *Geochimica et Cosmochimica Acta* 67:3735–3771.
- Greenwood R. C., Barrat J. A., Scott E. R., Haack H., Buchanan P. C., Franchi I. A., Yamaguchi A., Johnson D., Bevan A. W., and Burbine T. H. 2015. Geochemistry and oxygen isotope composition of main-group pallasites and olivine-rich clasts in mesosiderites: Implications for the “great dunite shortage” and HED-mesosiderite connection. *Geochimica et Cosmochimica Acta* 169:115–136.
- Gregory J. D., Mayne R. G., Boesenberg J. S., Humayun M., Silver A. P., Greenwood R. C., and Franchi I. A. 2016. Choteau makes three: A characterization of the third member of the Vermillion subgroup. *Lunar and Planetary Science Conference* 47:2393.
- Guignard J., Bystricky M., and Toplis M. J. 2012. Grain growth in forsterite-nickel mixtures: Analogues of small parent bodies during early accretion. *Physics of the Earth and Planetary Interiors* 204–205:37–51.
- Haag R. 2003. *The Robert Haag collection of meteorites*. Tucson, Arizona: Robert Haag Meteorites.
- Hsu W. 2003. Minor element zoning and trace element geochemistry of pallasites. *Meteoritics & Planetary Science* 38:1217–1241.
- Hughes J. M., Jolliff B. L., and Rakovan J. 2008. The crystal chemistry of whitlockite and merrillite and the dehydrogenation of whitlockite to merrillite. *American Mineralogist* 93:1300–1305.
- Jochum K. P., Hintenberger H., and Buchwald V. F. 1975. Distribution of minor and trace elements in the elongated troilite inclusions of the Cape York iron Agpallik. *Meteoritics* 10:419–421.
- Johnson D., Hutchison R., and Grady M. M. 2006a. Textural evidence for melt processes on the pallasite parent body. *Meteoritical Society Meeting* 69:5210.
- Johnson D., Hutchison R., Kirk C., and Grady M. M. 2006b. Hambleton—A new sulfur-rich pallasite. *Meteoritical Society Meeting* 69:5216.
- Jones R. H., Wasson J. T., Larson T., and Sharp Z. D. 2003. Milton: A new, unique pallasite. *Lunar and Planetary Science Conference* 34:1683.
- Kichanov S. E., Kozlenko D. P., Lukin E. V., Rutkauskas A. V., Krasavin E. A., Rozanov A. Y., and Savenko B. N. 2018. A neutron tomography study of the Seymchan pallasite. *Meteoritics & Planetary Science*. 53:2155–2164. <https://doi.org/10.1111/maps.13115>.
- Kiseeva E. S. and Wood B. J. 2013. A simple model for chalcophile element partitioning between sulphide and silicate liquids with geochemical applications. *Earth and Planetary Science letters* 383:68–81.
- Kissin S. A. 2008. Olivine morphology and the origin of main group pallasites. *Goldschmidt Conference Abstracts* 18:A476.

- Kissin S. A. 2009. Olivine morphology and trace element fractionation in metal of main group pallasites. AGU Spring Meeting Abstracts, abstract id. MA13A-04.
- Kissin S. A., MacRae N. D., and Keays R. R. 2013. Southampton, Canada's third pallasite. *Canadian Journal of Earth Sciences* 50:26–31.
- Klosterman M. J. and Buseck P. R. 1973. Structural analysis of olivine in pallasitic meteorites: Deformation in planetary interiors. *Journal of Geophysical Research* 78:7581–7588.
- Kolomeitseva L. N. 1975. Equilibrium conditions in pallasites. *Meteoritika* 34:52–56.
- Kracher A. 1983. Notes on the evolution of the IIIAB/Pallasite parent body. 14th Lunar and Planetary Science Conference, pp. 405–406.
- Kracher A. and Wasson J. T. 1982. The role of S in the evolution of the parental cores of the iron meteorites. *Geochimica et Cosmochimica Acta* 46:2419–2426.
- Kracher A., Kurat G., and Buchwald V. F. 1977. Cape York: The extraordinary mineralogy of an ordinary iron meteorite and its implication for the genesis of IIIAB irons. *Geochemical Journal* 11:207–217.
- Kruijer T. S., Touboul M., Fischer-Gödde M., Bermingham K. R., Walker R. J., and Kleine T. 2014. Protracted core formation and rapid accretion of protoplanets. *Science* 344:1150–1154.
- Lauretta D. S., Hill D. H., DellaGiustina D. N., and Killgore M. 2006. The Fukang pallasite: Evidence for non-equilibrium shock processing (abstract #2250). 37th Lunar and Planetary Science Conference. CD-ROM.
- Leitch C. A., Steele I. M., Hutcheon I. D., and Smith J. V. 1979. Minor elements in pallasites: Zoning in Springwater olivine. *Lunar and Planetary Science Conference* 10:716–718.
- Li Y. and Audétat A. 2012. Partitioning of V, Mn, Co, Ni, Cu, Zn, As, Mo, Ag, Sn, Sb, W, Au, Pb, and Bi between sulfide phases and hydrous basanite melt at upper mantle conditions. *Earth and Planetary Science Letters* 355–356:327–340.
- Lifshitz I. M. and Slyozov V. V. 1961. The kinetics of precipitation from supersaturated solid solutions. *Journal of Physics and Chemistry of Solids* 19:35–50.
- Lovering J. F. 1957. Pressures and temperatures within a typical parent meteorite body. *Geochimica et Cosmochimica Acta* 12:253–261.
- Lugmair G. W. and Shukolyukov A. 1998. Early solar system timescales according to <sup>53</sup>Mn–<sup>53</sup>Cr systematics. *Geochimica et Cosmochimica Acta* 62:2863–2886.
- Mason B. 1963. The pallasites. *American Museum Novitates* 2163:1–19.
- Matsui T., Karato S.-I., and Yokokura T. 1980. Stress histories retained in olivines from pallasite meteorites. *Proceedings of the Lunar and Planetary Science Conference* 11:1047–1054.
- Matzen A. K., Baker M. B., Beckett J. R., and Stolper E. M. 2011. Fe-Mg partitioning between olivine and high-magnesian melts and the nature of Hawaiian parental liquids. *Journal of Petrology* 52:1243–1263.
- McKibbin S. J., O'Neill H. St. C., Mallmann G., and Halfpenny A. 2013. LA-ICP-MS mapping of olivine from the Brahin and Brenham meteorites: Complex elemental distributions in the pallasite olivine precursor. *Geochimica et Cosmochimica Acta* 119:1–17.
- McKibbin S. J., Ireland T. R., Holden P., O'Neill H. St. C., and Mallmann G. 2016. Rapid cooling of planetesimal core-mantle reaction zones from Mn-Cr isotopes in pallasites. *Geochemical Perspectives Letters* 2:68–77.
- Mingaye J. C. H. 1916. Notes on the Molong meteorite. *Records of the Geological Survey of New South Wales* 9:161–165.
- Mittlefehldt D. W. 1999. Geochemistry and origin of pallasite olivines (abstract #1828). 30th Lunar and Planetary Science Conference. CD-ROM.
- Mittlefehldt D. W. 2005. Origin of main-group pallasites. *Meteoritics & Planetary Science Supplement* 40:5025.
- Mittlefehldt D. W. and Herrin J. S. 2010. Trace element compositions of pallasite olivine grains and pallasite origin. *Meteoritical Society Meeting* 73:5386.
- Mittlefehldt D. W. and Rumble D. III. 2006. Geochemistry of pallasite olivines and the origin of main-group pallasites. *Meteoritics & Planetary Science Supplement* 41:5332.
- Mittlefehldt D. W., McCoy T. J., Goodrich C. A., and Kracher A. 1998. Non-chondritic meteorites from asteroidal bodies. In *Planetary materials*, edited by Papike J. J. *Reviews in Mineralogy*, vol. 36. Washington, D.C.: Mineralogical Society of America, pp. 4–1–4–195.
- Miyamoto M. 1997. Chemical zoning of olivine in several pallasites. *Journal of Geophysical Research* 102:21,613–21,618.
- Mori H. 1986. Dislocation substructures of olivine crystals from pallasite meteorites. 17th Lunar and Planetary Science Conference, pp. 571–572.
- Mullane E., Alard O., Gounelle M., and Russell S. S. 2004. Laser ablation ICP-MS study of IIIAB irons and pallasites: Constraints on the behaviour of highly siderophile elements during and after planetesimal core formation. *Chemical Geology* 208:5–28.
- Mysen B. 2007. Partitioning of calcium, magnesium, and transition metals between olivine and melt governed by the structure of the silicate melt at ambient pressure. *American Mineralogist* 92:844–862.
- Nichols C. I. O., Bryson J. F. J., Herrero-Albillos J., Kronast F., Nimmo F., and Harrison R. J. 2016. Pallasite paleomagnetism: Quiescence of a core dynamo. *Earth and Planetary Science Letters* 441:103–112.
- Ohtani E. 1983. Formation of olivine textures in pallasites and thermal history of pallasites in their parent body. *Physics of the Earth and Planetary Interiors* 32:182–192.
- Olsen E. and Fredriksson K. 1966. Phosphates in iron and pallasite meteorites. *Geochimica et Cosmochimica Acta* 30:459–470.
- Olsen E. and Fuchs L. H. 1967. The state of oxidation of some iron meteorites. *Icarus* 6:242–253.
- Olsen E. J., Kracher A., Davis A. M., Steele I. M., Hutcheon I. D., and Bunch T. E. 1999. The phosphates of IIIAB iron meteorites. *Meteoritics & Planetary Science* 34:285–300.
- Pellas P., Perron C., Crozaz G., Perelygin V. P., and Stetsenko S. G. 1983. Fission track age and cooling rate of the Marjalahti pallasite. *Earth and Planetary Science Letters* 64:319–326.
- Prior G. T. 1916. On the genetic relationship and classification of meteorites. *Mineralogical Magazine* 18:26–44.
- Prissel T. C., Gross J., and Draper D. S. 2017. Application of olivine-spinel equilibria to extraterrestrial igneous systems (abstract #2436). 48th Lunar and Planetary Science Conference. CD-ROM.
- Putirka K. D. 2005. Mantle potential temperatures at Hawaii, Iceland, and the mid-ocean ridge system, as inferred from olivine phenocrysts: Evidence for thermally driven mantle

- plumes. *Geochemistry Geophysics Geosystems* 6:1–14. Q05L08https://doi.org/10.1029/2005GC000915.
- Putirka K. 2016. Rates and styles of planetary cooling on Earth, Moon, Mars, and Vesta, using new models for oxygen fugacity, ferric-ferrous ratios, olivine-liquid Fe-Mg exchange, and mantle potential temperature. *American Mineralogist* 101:819–840.
- Quitté G., Birck J.-L., and Allègre C. J. 2005. Stony-iron meteorites: History of the metal phase according to tungsten isotopes. *Geochimica et Cosmochimica Acta* 69:1321–1332.
- Raghavan V. 1988. The Fe-P-S system. In *Phase diagrams of ternary iron alloys 2*. New Delhi, India: Indian National Scientific Documentation Centre. pp. 209–217.
- Raghavan V. 2004. Fe-Ni-S (Iron-Nickel-Sulfur). *Journal of Phase Equilibria and Diffusion* 25:373–381.
- Righter K., Arculus R. J., Delano J. W., and Paslick C. 1990. Electrochemical measurements and thermodynamic calculations of redox equilibria in pallasite meteorites: Implications for the eucrite parent body. *Geochimica et Cosmochimica Acta* 54:1803–1815.
- Sadilenko D. A., Borisovskiy S. E., Korochantsev A. V., Abdrakhimov A. M., Ivanova M. A., and Zhuravlev D. I. 2006. Discovery, petrography, mineralogy, and chemistry of Pallasovka, a new pallasite from Russia. *Lunar and Planetary Science* 37:1623.
- Saiki K., Laporte D., Vielzeuf D., Nakashima S., and Boivin P. 2003. Morphological analysis of olivine grains annealed in an iron-nickel matrix: Experimental constraints on the origin of pallasites and on the thermal history of their parent bodies. *Meteoritics & Planetary Science* 38:427–444.
- Sanborn M. E. and Yin Q.-Z. 2014. Chromium isotopic composition of the anomalous eucrites: An additional geochemical parameter for evaluating their origin. *Lunar and Planetary Science Conference* 45:2018.
- Schürmann E. and Neubert V. 1980. Schmelzgleichgewichte in den eisenreichen Ecken der Dreistoffsysteme Eisen-Schwefel-Kohlenstoff, Eisen-Schwefel-Phosphor und Eisen-Schwefel-Silizium. *Giessereiforschung* 32:1–5.
- Schürmann E. and Schäfer K. 1968. Schmelzgleichgewichte in den Dreistoffsystemen Eisen-Schwefel-Kohlenstoff, Eisen-Schwefel-Phosphor und Eisen-Schwefel-Silizium. *Giessereiforschung* 24:21–33.
- Scott E. R. D. 1977a. Pallasites—Metal composition, classification and relationships with iron meteorites. *Geochimica et Cosmochimica Acta* 41:349–360.
- Scott E. R. D. 1977b. Formation of olivine-metal textures in pallasite meteorites. *Geochimica et Cosmochimica Acta* 41:693–710.
- Scott E. R. D. 2007. Impact origin for pallasites. *Lunar and Planetary Science Conference* 38:2284.
- Scott E. R. D. 2017. Pallasites: Olivine-metal textures, metal compositions, minor phases, origins, and insights into processes at core-mantle boundaries of asteroids. *Lunar and Planetary Science Conference* 48:1037.
- Scott E. R. D., Greenwood R. C., Franchi I. A., and Sanders I. S. 2009. Oxygen isotopic constraints on the origin and parent bodies of eucrites, diogenites, and howardites. *Geochimica et Cosmochimica Acta* 73:5835–5853.
- Sharygin V. V., Kovyazin S. V., and Podgornykh N. M. 2006. Mineralogy of olivine-hosted inclusions from the Omolon pallasite (abstract #1235). 37th Lunar and Planetary Science Conference. CD-ROM.
- Shen J. J., Papanastassiou D. A., and Wasserburg G. J. 1998. Re-Os systematics in pallasite and mesosiderite metal. *Geochimica et Cosmochimica Acta* 62:2715–2723.
- Shima M., Okada A., and Yabuki H. 1980. Mineralogical and Petrographical study of the Zaisho meteorite: A pallasite from Japan. *Zeitschrift für Naturforschung A* 35:64–68.
- Smith J. V., Steele I. M., and Leitch C. A. 1983. Mineral chemistry of the shergottites, nakhlites, Chassigny, Brachina, pallasites and ureilites. Proceedings of the Fourteenth Lunar and Planetary Science Conference, Part 1. *Journal of Geophysical Research* 88 (suppl.):B229–B236.
- Solferino G. F. D., Golabek G. J., Nimmo F., and Schmidt M. W. 2015. Fast grain growth of olivine in liquid Fe–S and the formation of pallasites with rounded olivine grains. *Geochimica et Cosmochimica Acta* 162:259–275.
- Sonzogni Y., Devouard B., Provost A., and Devidal J.-L. 2009. Olivine-hosted melt inclusions in the Brahni pallasite (abstract #5070). 72nd Annual Meeting of the Meteoritical Society. *Meteoritics & Planetary Science* 44. *Meteoritical Society Meeting* 72:5070.
- Spinsby J., Friedrich H., and Buseck P. R. 2008. Volume and surface-area measurements using tomography, with an example from the Brenham pallasite meteorite. *Computers and Geosciences* 34:1–7.
- Starykh R. V. and Sineva S. I. 2012. Study of the liquidus and solidus surfaces of the quaternary Fe–Ni–Cu–S system: V. Refinement and addition of the data on the ternary Fe–Ni–S and Fe–Ni–Cu phase diagrams. *Russian Metallurgy* 3:189–194.
- Steele I. M. 1994. Chemical zoning and exsolution in olivine of the Pavlodar pallasite: Comparison with Springwater olivine. 25th Lunar and Planetary Science Conference. pp. 1335–1336.
- Suzuki A. M., Yasuda A., and Ozawa K. 2008. Cr and Al diffusion in chromite spinel: Experimental determination and its implication for diffusion creep. *Physics and Chemistry of Minerals* 35:433–445.
- Takeda H., Miyamoto M., Yanai K., and Haramura H. 1978. A preliminary mineralogical examination of the Yamato-74 achondrites. *Memoirs of the National Institute of Polar Research, Special Issue* 8:170–184.
- Tarduno J. A., Cottrell R. D., Nimmo F., Hopkins J., Voronov J., Erickson A., Blackman E., Scott E. R. D., and McKinley R. 2012. Evidence for a dynamo in the main group pallasite parent body. *Science* 338:939–942.
- Toplis M. J. 2005. The thermodynamics of iron and magnesium partitioning between olivine and liquid: Criteria for assessing and predicting equilibrium in natural and experimental systems. *Contributions to Mineralogy and Petrology* 149:22–39.
- Ulf-Møller F. 1998a. Effects of liquid immiscibility on trace element fractionation in magmatic iron meteorites: A case study of group IIIAB. *Meteoritics & Planetary Science* 33:207–220.
- Ulf-Møller F. 1998b. Solubility of chromium and oxygen in metallic liquids and the co-crystallization of chromite and metal in iron meteorite parent bodies. (abstract #1969). 29th Lunar and Planetary Science Conference. CD-ROM.
- Ulf-Møller F., Choi B.-G., Rubin A. E., Tran J., and Wasson J. T. 1998. Paucity of sulfide in a large slab of Esquel: New perspectives on pallasite formation. *Meteoritics & Planetary Science* 33:221–227.
- Van Niekerk D., Greenwood R. C., and Franchi I. A. 2007. Seymchan: A main group pallasite—Not an iron meteorite

- (abstract #5196). 70th Annual Meeting of the Meteoritical Society. *Meteoritics & Planetary Science* 42.
- Van Orman J. A. and Crispin K. L. 2010. Diffusion in oxides. *Reviews in Mineralogy & Geochemistry* 72:757–825.
- Van Roosbroek N., Pittarello L., Hamann C., Greshake A., Debaille V., Wirth R., and Claeys P. 2015. First findings of impact melt in the IIE Netschaëvo meteorite. *Goldschmidt Abstracts* 3241.
- Van Roosbroek N., Hamann C., McKibbin S., Greshake A., Wirth R., Pittarello L., Hecht L., Claeys P., and Debaille V. 2017. Immiscible silicate liquids and phosphoran olivine in Netschaëvo IIE silicate: Analogue for planetesimal core-mantle boundaries. *Geochimica et Cosmochimica Acta* 197:378–395.
- Vogt K., Dohmen R., and Chakraborty S. 2015. Fe-Mg diffusion in spinel: New experimental data and a point defect model. *American Mineralogist* 100:2112–2122.
- Wagner C. 1961. Theorie der Alterung von Niederschlägen durch Umlösen (Ostwald-Reifung). *Zeitschrift für Elektrochemie* 65:581–591.
- Wahl W. 1965. The pallasite problem. *Geochimica et Cosmochimica Acta* 29:177–181.
- Wan Z., Coogan L. A., and Canil D. 2008. Experimental calibration of aluminum partitioning between olivine and spinel as a geothermometer. *American Mineralogist* 93:1142–1147.
- Wang Y., Hua X., and Hsu W. 2006. Phosphoran olivine in opaque assemblages of the Ningqiang carbonaceous chondrite: Implications to their precursors (abstract #1504). 37th Lunar and Planetary Science Conference. CD-ROM.
- Ward D., Bischoff A., Roszjar J., Berndt J., and Whitehouse M. J. 2017. Trace element inventory of meteoritic Ca-phosphates. *American Mineralogist* 102:1856–1880.
- Warren P. H. 2011. Stable-isotopic anomalies and the accretionary assemblage of the Earth and Mars: A subordinate role for carbonaceous chondrites. *Earth and Planetary Science Letters* 311:93–100.
- Wasson J. T. 2016. Formation of the Treysa quintet and the main-group pallasites by impact-generated processes in the IIIAB asteroid. *Meteoritics & Planetary Science* 51:773–784.
- Wasson J. T. and Choi B.-G. 2003. Main-group pallasites: Chemical composition, relationship to IIIAB irons, and origin. *Geochimica et Cosmochimica Acta* 67:3079–3096.
- Wasson J. T., Lange D. E., Francis C. A., and Ulff-Møller F. 1999. Massive chromite in the Brenham pallasite and the fractionation of Cr during the crystallization of asteroidal cores. *Geochimica et Cosmochimica Acta* 63:1219–1232.
- Wilson L. and Keil K. 2017. Arguments for the non-existence of magma oceans in asteroids. In *Planetesimals: Early differentiation and consequences for planets*, edited by Elkins-Tanton L. and Weiss B. Cambridge: Cambridge University Press. pp. 159–179.
- Yang J. and Goldstein J. I. 2006. Metallographic cooling rates of the IIIAB iron meteorites. *Geochimica et Cosmochimica Acta* 70:3197–3215.
- Yang J., Goldstein J. I., and Scott E. R. D. 2010. Main-group pallasites: Thermal history, relationship to IIIAB irons, and origin. *Geochimica et Cosmochimica Acta* 74:4471–4492.
- Yoshikawa M. and Matsueda H. 1992. Texture, chemical composition and genesis of schreibersite in iron meteorite. *Journal of the Faculty of Science, Hokkaido University. Series 4, Geology and Mineralogy* 23:255–280.
- Zhou Y. and Steele I. M. 1993. Chemical zoning and diffusion of Ca, Al, Mn, and Cr in olivine of Springwater pallasite. *Lunar and Planetary Science Conference* 24:1573–1574.
- Zucchini A., Petrelli M., Frondini F., Petrone C. M., Sassi P., Di Michele A., Palmerini S., Trippella O., and Busso M. 2018. Chemical and mineralogical characterization of the Mineo (Sicily, Italy) pallasite: A unique sample. *Meteoritics & Planetary Science* 53:268–283.
- Zucolotto M. E. 2000. Quijingue, Bahia, the first Brazilian pallasite (abstract). *Meteoritics & Planetary Science* 35: A179.

## SUPPORTING INFORMATION

Additional supporting information may be found in the online version of this article:

**Data S1.** New EMPA data for PMG olivine, and summary of olivine Mg-Fe-Mn systematics, macroscopic petrographic textures, phosphate mineralogy, and chromite compositions.